Effects of Quadratic Singular Curves in Integrable Equations

By Aiyong Chen, Shuangquan Wen, Shengqiang Tang, Wentao Huang, and Zhijun Qiao

In this paper, the effects of quadratic singular curves in integrable wave equations are studied by using the bifurcation theory of dynamical system. Some new singular solitary waves (pseudo-cuspons) and periodic waves are found more weak than regular singular traveling waves such as peaked soliton (peakon), cusp soliton (cuspon), cusp periodic wave, etc. We show that while the first-order derivatives of the new singular solitary wave and periodic waves exist, their second-order derivatives are discontinuous at finite number of points for the solitary waves or at infinitely countable points for the periodic wave. Moreover, an intrinsic connection is constructed between the singular traveling waves and quadratic singular curves in the phase plane of traveling wave system. The new singular periodic waves, pseudo-cuspons, and compactons emerge if corresponding periodic orbits or homoclinic orbits are tangent to a hyperbola, ellipse, and parabola. In particular, pseudo-cuspon is proposed for the first time. Finally, we study the qualitative behavior of the new singular solitary wave and periodic wave solutions through theoretical analysis and numerical simulation.

1. Introduction

Mathematical modeling of dynamical systems processing in a great variety of natural phenomena usually leads to nonlinear partial differential equations (PDEs). There is a special class of solutions for nonlinear PDEs that are of

Address for correspondence: Zhijun Qiao, Department of Mathematics, University of Texas-Pan American, Edinburg, TX 78541, USA; e-mail: qiao@utpa.edu

DOI: 10.1111/sapm.12060

STUDIES IN APPLIED MATHEMATICS 00:1–38

considerable interest, namely, the traveling wave solutions. Such a wave may be localized or periodic, which propagates at constant speed without changing its shape.

Many powerful methods have been presented for finding the traveling wave solutions, such as the Bäcklund transformation [1], tanh-coth method [2], bilinear method [3], symbolic computation method [4], Lie group analysis method [5], and so on. Furthermore, a great amount of works focused on various extensions and applications of the methods to simplify the calculation procedure. The basic idea of those methods is that, by introducing different types of Ansatz, the original PDEs can be transformed into a set of algebraic equations. Balancing the same order of the Ansatz then yields explicit expressions for the PDE waves. However, not all of the special forms for the PDE waves can be derived by those methods. To obtain all possible forms of the PDE waves and analyze qualitative behaviors of solutions, the bifurcation theory plays a very important role in studying the evolution of wave patterns with variation of parameters [6–16]. Moreover, an attractive classification is given for solitary wave bifurcations in generalized nonlinear Schrodinger equations in Ref. [17].

To study the traveling wave solutions of a nonlinear PDE

$$\Phi(u, u_t, u_x, u_{xx}, u_{xt}, u_{tt}, \cdots) = 0, \tag{1}$$

let $\xi = x - ct$, $u(x, t) = \varphi(\xi)$, where c is the wave speed. Substituting them into (1) leads the PDE to the following ordinary differential equation:

$$\Phi_1(\varphi, \varphi', \varphi'', \cdots) = 0. \tag{2}$$

Here, we consider the case of (2), which can be reduced to the following planar dynamical system:

$$\frac{d\varphi}{d\xi} = \varphi' = y, \quad \frac{dy}{d\xi} = F(\varphi, y), \tag{3}$$

through several times integrals. Equation (3) is called the traveling wave system of the nonlinear PDE (1). Thus, we just study the traveling wave system (3) to get the traveling wave solutions of the nonlinear PDE (1).

Let us begin with some well-known nonlinear wave equations. The first one is the Camassa–Holm (CH) equation

$$u_t - u_{txx} + 3uu_x = 2u_x u_{xx} + uu_{xxx}, \tag{4}$$

arising as a model for nonlinear waves in cylindrical axially symmetric hyperelastic rods, with $u(x, t)$ representing the radial stretch relative to a prestressed state [18] where Camassa and Holm showed that Equation (4) has a peakon of the form $u(x, t) = ce^{-|x-ct|}$. Among the nonanalytic entities,

the peakon, a soliton with a finite discontinuity in gradient at its crest, is perhaps the weakest nonanalyticity observable by the eye [19]. However, in this paper, we provide new singular solitary waves (pseudo-cuspons) with weaker singularity than peakon.

To understand the role of nonlinear dispersion in the formation of patters in liquid drop, Rosenau and Hyman [20] introduced and studied a family of fully nonlinear dispersion Korteweg–de Vries equations

$$u_t + (u^m)_x + (u^n)_{xxx} = 0. \tag{5}$$

This equation, denoted by $K(m, n)$, owns the property that for certain m and n, its solitary wave solutions have compact support [20]. That is, they identically vanish outside a finite core region. For instance, the $K(2, 2)$ equation admits the following compacton solution:

$$u(x,t) = \begin{cases} \frac{4c}{3}\cos^2(\frac{x-ct}{4}), & |x-ct| \le 2\pi, \\ 0, & \text{otherwise.} \end{cases} \tag{6}$$

The Camassa–Holm equation, the $K(2,2)$ equation, and almost all integrable dispersive equations have the same class of traveling wave systems, which can be written in the following form:

$$\begin{cases} \frac{d\varphi}{d\xi} = y = \frac{1}{D^2(\varphi)}\frac{\partial H}{\partial y}, \\ \frac{dy}{d\xi} = -\frac{1}{D^2(\varphi)}\frac{\partial H}{\partial \varphi} = -\frac{D'(\varphi)y^2+g(\varphi)}{D^2(\varphi)}, \end{cases} \tag{7}$$

where $H = H(\varphi, y) = \frac{1}{2}y^2D^2(\varphi) + \int D(\varphi)g(\varphi)d\varphi$ is the first integral. It is easy to see that Equation (4) is actually a special case of (3) with $F(\varphi, y) = -\frac{1}{D^2(\varphi)}\frac{\partial H}{\partial \varphi}$. If there is a function $\varphi = \varphi_s$ such that $D(\varphi_s) = 0$, then $\varphi = \varphi_s$ is a vertical straight line solution of the system

$$\begin{cases} \frac{d\varphi}{d\zeta} = yD(\varphi), \\ \frac{dy}{d\zeta} = -D'(\varphi)y^2 - g(\varphi), \end{cases} \tag{8}$$

where $d\xi = D(\varphi)d\zeta$ for $\varphi \neq \varphi_s$. The two systems have the same topological phase portraits except for the vertical straight line $\varphi = \varphi_s$ and the directions in time. Consequently, we can obtain bifurcation and smooth solutions of the nonlinear PDE (1) through studying the system (8), if the corresponding orbits are bounded and do not intersect with the vertical straight line $\varphi = \varphi_s$. However, the orbits, which do intersect with the vertical straight line $\varphi = \varphi_s$ or are unbounded but can approach the vertical straight line, correspond to the nonsmooth singular traveling waves [8–13]. It is worth pointing out that traveling waves sometimes lose their smoothness during the propagation due

to the existence of singular curves within the solution surfaces of the wave equation.

The relationships, between the traveling waves of the nonlinear PDEs with a singularity of vertical straight line and the orbits of the corresponding traveling wave systems, are well known [21–29]. However, till now there are few works on the integrable PDEs with the following types of singular curves:

$$\frac{d\varphi}{d\xi} = y, \quad \frac{dy}{d\xi} = F(\varphi, y) = \frac{P(\varphi, y)}{Q(\varphi, y)}, \tag{9}$$

where the functions $P(\varphi, y)$ and $Q(\varphi, y)$ satisfy $y\frac{\partial Q(\varphi,y)}{\partial \varphi} + \frac{\partial P(\varphi,y)}{\partial y} \equiv 0$, that is, this is a first integral of system (9). Obviously, $Q(\varphi, y) = 0$ defines a set of real planar curves such that the right-hand side of the second equation of the system (9) is not well defined on these curves, which form singular curves of the corresponding nonlinear PDEs. What kinds of traveling wave solution will be achieved for the presence of the singular curves for a given nonlinear wave equation, still needs a further study. For the following nonlinear wave equations, the singular equation $Q(\varphi, y) = 0$ are required to be a quadratic curve such as hyperbola, ellipse, and parabola.

In 1995 and 1996, Fokas [36], and Olver and Rosenau [34] studied the symmetry and tri-Hamiltonian structure of the following cubic Camassa–Holm type equation:

$$m_t = au_x + \frac{1}{2}[(u^2 - u_x^2)m]_x, \quad m = u - u_{xx}, \tag{10}$$

where $a(\neq 0)$ is a constant. The equation is obtained through a reshuffling procedure of the Hamiltonian operators underlying the bi-Hamiltonian structure of mKdV equations. In [19], Rosenau pointed out that the interaction of nonlinear dispersion with nonlinear convection generates exactly compact structures. Unfortunately, as the author has pointed in [19], "a lack of proper mathematical tools makes this goal at the present time pretty much beyond our reach." Recently, Chen et al. studied the dynamical system and phase portrait of Equation (10) with providing W-/M-shaped solitary wave solutions in [30], and Qiao and Li gave the Lax pair and nonsmooth solitons in an explicit form including W-/M-shaped solitons.

In 2006, the author in [31] investigated the following completely integrable wave equation, which is now called the Fokas-Olver-Rosenau-Qiao (FORQ) equation or the modified CH equation:

$$m_t + m_x(u^2 - u_x^2) + 2m^2u_x, \quad m = u - u_{xx}, \tag{11}$$

with giving Lax pair, the W-/M-shape solitons, and cuspons. This equation can also be derived from the two-dimensional (2D) Euler equation by using

the approximation procedure, which might imply its water wave background. Recently, Qiao et al. [44] proposed a generalized integrable Camassa–Holm equation with both quadratic and cubic nonlinearity

$$m_t = bu_x + \frac{1}{2}k_1[(u^2 - u_x^2)m]_x + \frac{1}{2}k_2(2mu_x + m_x u), \quad m = u - u_{xx}, \quad (12)$$

and presented the Lax pair, bi-Hamiltonian structure, and multipeakon solutions to the Equation (12). In Refs. [32, 33], Li and his coauthors studied the existence of breaking wave solutions of the Equations (10)–(12). For those equations, it is not difficult for one to find that the corresponding traveling wave system (3) possess hyperbolas as singular curves in the phase plane. Also, there exists a clear connection between the breaking wave solutions and singular curves. In this paper, we study further effects of hyperbolas as singular curves for the integrable wave equations, and provide new singular periodic waves and singular solitons (pseudo-cuspons).

In 1997, Rosenau [19] studied the nonanalytic solitary waves of the following integrable wave equation:

$$m_t = au_x + \frac{1}{2}[(u^2 + u_x^2)m]_x, \qquad m = u + u_{xx}, \quad (13)$$

which appeared in Fokas [36] and Olver and Rosenau [34]. For our convenience, let us call it the Fokas-Olver-Rosenau (FOR) equation. In [35], the authors find that, in comparison with the $K(m,n)$ equation, the FOR equation has double compactons for some suitably chosen parameters. Actually in 1995, Fokas [36] proposed the following large class of physically integrable equations in the form of:

$$u_t + u_x + \nu u_{xxt} + \beta u_{xxx} + \alpha u u_x + \frac{1}{3}\nu\alpha(u u_{xxx} + 2u_x u_{xx}) + 3\mu\alpha^2 u^2 u_x$$

$$+ \nu\mu\alpha^2(u^2 u_{xxx} + u_x^3 + 4u u_x u_{xx}) + \nu^2\mu\alpha^2(u_x^2 u_{xxx} + 2u_x u_{xx}^2) = 0. \quad (14)$$

Li and Zhang [37] considered the existence of solitary wave, kink and antikink wave solutions, and uncountably infinite smooth and nonsmooth periodic wave solutions of Equation (14) by using the bifurcation theory of dynamical systems. Bi [38] studied singular solitary waves associated with homoclinic orbits by considering the effects of quadratic singular curves. For Equations (13) and (14), we find that the corresponding traveling wave system (3) possesses elliptic singular curves in the phase plane. In this paper, we consider the effects of elliptic singular curves for those wave equations toward getting new singular periodic waves and compactons.

In 2003, Manna and Neveu [39] derived the following integrable model from asymptotic dynamics of a short capillary-gravity wave

$$u_{xt} = \frac{3g(1-3\theta)}{2vh}u - \frac{1}{2}uu_{xx} - \frac{1}{4}u_x^2 + \frac{3h^2}{4v}u_{xx}u_x^2, \tag{15}$$

where $u(x, t)$ is the fluid velocity on the surface, x and t are space and time variables. After appropriately rescaling of the variables, one can bring Equation (15) into the form of

$$u_{xt} = u - uu_{xx} - \frac{1}{2}u_x^2 + \frac{\lambda}{2}u_{xx}u_x^2, \tag{16}$$

where λ is expressed in terms of the physical parameters from Equation (15).

The Hunter–Saxton (HS) equation [45]

$$(u_t + uu_x)_x = \frac{1}{2}u_x^2, \tag{17}$$

is an integrable PDE that arises in the study of massive nematic liquid crystals and shallow water waves, and has been already extended to a completely integrable hierarchy through the Lax pair procedure [46]. In 2004, Brunelli et al. [40] discussed the deformed Hunter–Saxton (DHS) equation

$$u_{xxt} = \alpha u_x - 2u_xu_{xx} - uu_{xxx} + \frac{\lambda}{6}(u_x^3)_{xx}, \tag{18}$$

regarding integrability, etc. For Equations (16) and (18), we find that the corresponding traveling wave system (3) possesses parabolic singular curves in the phase plane, which is the first time, within our knowledge, appearing in study of traveling wave dynamics.

The whole paper is organized as follows. In Section 2, we define pseudo-cuspon and discuss the difference among peakons, cuspons, and pseudo-cuspons. In Section 3, we investigate the hyperbolic singular curves for singular periodic waves and singular solitary waves of the FORQ equation (11). In Section 4, we study the the elliptic singular curves and compactons for the FOR Equation (13). In Section 5, we analyze the effects of parabolic singular curves for the DHS equation (18). A short conclusion is given in Section 6.

2. Solitary wave solutions with singularities

The existence of peakon is of interest for nonlinear wave equations because most integrable models have smooth solitons. The first-order derivative of peakon does not exist at a finite number of points where the jump of the

derivative is finite. Cuspon is another type of continuous solitary waves with an infinite jump for the first-order derivative at its crest. Both peakons and cuspons are closely related to the singular straight lines of corresponding traveling wave systems. To compare the difference between the effect of singular straight lines and the one of quadratic singular curves for integrable equations, let us consider the occurrence of peakons and cuspons by using the phase space analysis technique.

DEFINITION 1. *A wave function $u(\xi)$ is called a peakon if $u(\xi)$ is globally continuous and bounded and locally smooth on both sides of ξ_0 and* $\lim_{\xi\uparrow\xi_0} u_\xi(\xi) = -\lim_{\xi\downarrow\xi_0} u_\xi(\xi) = a, a \neq 0, a \neq \pm\infty$.

DEFINITION 2. *A wave function $u(\xi)$ is called a cuspon if $u(\xi)$ is globally continuous and bounded and locally smooth on both sides of ξ_0 and* $\lim_{\xi\uparrow\xi_0} u_\xi(\xi) = -\lim_{\xi\downarrow\xi_0} u_\xi(\xi) = \pm\infty$.

The concept of peakon and cuspon can also be seen in Ref. 28. In this paper, we propose a new singular solitary wave solution with discontinuous second-order derivative, which is called pseudo-cuspon below.

DEFINITION 3. *A wave function $u(\xi)$ is called a pseudo-cuspon if $u(\xi)$, $u_\xi(\xi)$ are globally continuous and bounded and $u_\xi(\xi)$ is locally smooth on both sides of ξ_0 and* $\lim_{\xi\uparrow\xi_0} u_{\xi\xi}(\xi) = -\lim_{\xi\downarrow\xi_0} u_{\xi\xi}(\xi) = \pm\infty$.

Case 1. Peakon

In the study of nonanalytic traveling waves, peakon is perhaps the simplest and best-known solitary wave. Let us first discuss the CH peakons. Let $u(x,t) = \varphi(\xi)$ $(\xi = x - ct)$ be a solution of the CH Equation (4), then it follows that

$$-c\varphi' + c\varphi''' + 3\varphi\varphi' = 2\varphi'\varphi'' + \varphi\varphi'''. \tag{19}$$

Integration yields

$$-c\varphi + c\varphi'' + \frac{3}{2}\varphi^2 = \varphi\varphi'' + \frac{1}{2}(\varphi')^2 + g, \tag{20}$$

where g is an integral constant. Clearly, Equation (20) is equivalent to the following 2D system

$$\begin{cases} \frac{d\varphi}{d\xi} = y, \\ \frac{dy}{d\xi} = \frac{\frac{3}{2}\varphi^2 - c\varphi - g - \frac{1}{2}y^2}{\varphi - c}, \end{cases} \tag{21}$$

which has the first integral

$$H(\varphi, y) = (\varphi - c)\left(\frac{1}{2}y^2 - \frac{1}{2}(\varphi - c)^2 - c(\varphi - c) - \frac{c^2 - 2g}{2}\right). \tag{22}$$

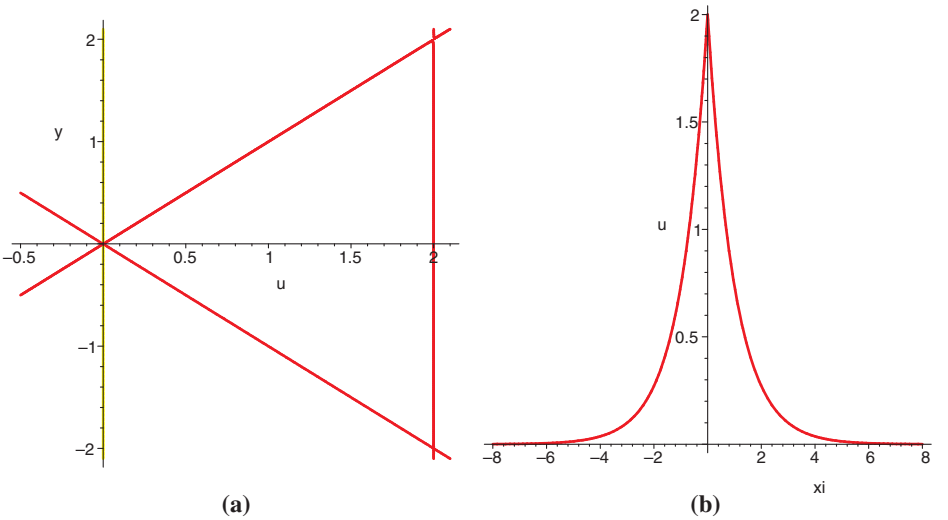

Figure 1. (a) The heteroclinic orbits $H(\varphi, y) = 0$ defined by (22). (b) The profile of a peakon.

Let $d\xi = (\varphi - c)d\zeta$, then the 2D system (21) becomes

$$\begin{cases} \frac{d\varphi}{d\zeta} = (\varphi - c)y, \\ \frac{dy}{d\zeta} = \frac{3}{2}\varphi^2 - c\varphi - g - \frac{1}{2}y^2. \end{cases} \tag{23}$$

If $g = 0, c > 0$, there is a family of periodic orbits enclosing the center point $(\frac{2c}{3}, 0)$, and the family of periodic orbits is surrounded by a triangle consisting of three heteroclinic straight line orbits containing the saddle points $(0, 0)$ and $(c, \pm c)$. The topological phase portrait of the 2D system (21) in the (φ, y)-plane is shown in Figure 1(a). The orbit defined by $H(\varphi, y) = 0$ has two intersection points with the singular line $\varphi = c$. From the algebraic equation $y = \pm\varphi$ of the orbit, we may obtain the parametric representation of the following peakon solution:

$$\varphi(\xi) = ce^{-|\xi|}, \tag{24}$$

with the properties:

$$\varphi(0) = c, \quad \varphi(\pm\infty) = 0, \quad \varphi'(0+) = -c, \quad \varphi'(0-) = c.$$

Clearly, the first-order derivative of $\varphi(\xi)$ does not exist at $\xi = 0$. The profile of peakon wave is shown in Figure 1(b).

Case 2. Cuspon

Cuspon is another type of continuous solitary waves, but the first-order derivative is discontinuous at its crest with an infinite jump.

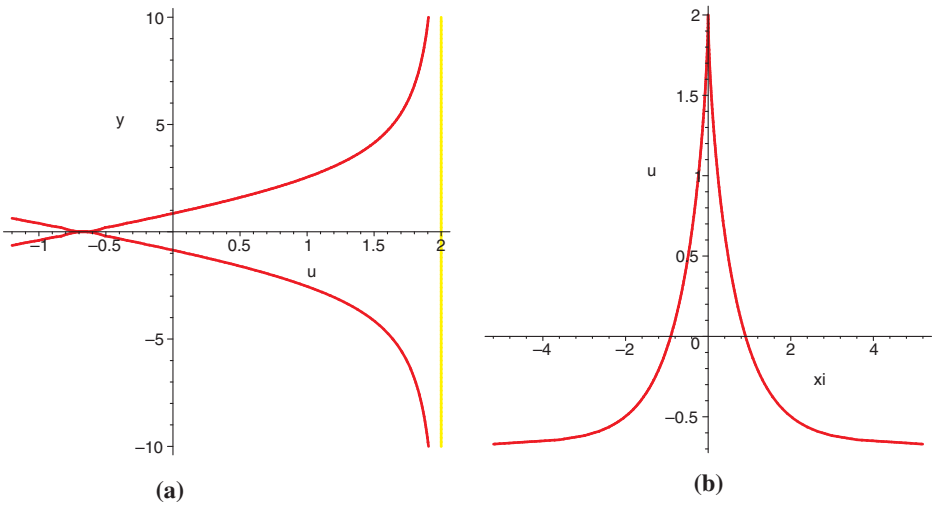

Figure 2. (a) Two open curves of the system (21). (b) The profile of a cuspon.

Let us still use the CH equation as an example. If $c > 0$ and $g = \frac{c^2}{2}$, the equilibrium point $(-\frac{c}{3}, 0)$ is a saddle point. Let l^s and l^u denote stable and unstable manifolds for the saddle point $(-\frac{c}{3}, 0)$ (see Figure 2(a)), respectively. The orbits l^s and l^u are determined by the algebraic curve

$$y^2 = \frac{(\varphi + \frac{c}{3})^2(\varphi - \frac{5c}{3})}{\varphi - c}. \tag{25}$$

If $\varphi(0) = c$, then from (25) and the first equation of (21) we obtain the following parametric representations of a cuspon:

$$I_1(\varphi) - \frac{\sqrt{6}}{3} I_2(\varphi) = |\xi| + \ln c - \frac{\sqrt{6}}{3} \ln(6c), \tag{26}$$

where

$$I_1(\varphi) = \ln|3\varphi - 4c + \sqrt{3(3\varphi - 5c)(\varphi - c)}|, \tag{27}$$

$$I_2(\varphi) = \ln\left|\frac{6c(19c - 15\varphi - 6\sqrt{2(3\varphi - 5c)(\varphi - c)})}{3\varphi + c}\right|. \tag{28}$$

Equation (25) implies

$$\varphi(\pm\infty) = -\frac{c}{3}, \quad \varphi'(0+) = +\infty, \quad \varphi'(0-) = -\infty.$$

Thus, the first-order derivative of the cuspon wave solution $\varphi(\xi)$ at $\xi = 0$ has an infinite jump from $-\infty$ to $+\infty$. The profile of cuspon wave is shown in Figure 2(b).

Case 3. Pseudo-cuspon

Cuspon admits discontinuous first-order derivative at its crest. However, pseudo-cuspon is smooth up to the first-order derivative and its second-order derivative is discontinuous at its crest. Let us pick Equation (10) as an example. Substituting $u = u(x - ct) = \varphi(\xi)$ into Equation (10) leads to

$$-c(\varphi - \varphi'')' = a\varphi' + \frac{1}{2}[(\varphi^2 - \varphi'^2)(\varphi - \varphi'')]'. \tag{29}$$

Integrating (29) once and taking the integration constant as zero, we have

$$(\varphi^2 - \varphi'^2 + 2c)\varphi'' = \varphi^3 + 2(a + c)\varphi - \varphi\varphi'^2. \tag{30}$$

Clearly, Equation (30) is equivalent to the following 2D system:

$$\begin{cases} \frac{d\varphi}{d\xi} = y, \\ \frac{dy}{d\xi} = \frac{\varphi(\varphi^2 - y^2 + 2(a+c))}{\varphi^2 - y^2 + 2c}, \end{cases} \tag{31}$$

which has the first integral

$$H(\varphi, y) = (y^2 - \varphi^2 - 2c)^2 + 4a\varphi^2 = h. \tag{32}$$

Apparently, the system (31) has a hyperbolic singular curve $\varphi^2 - y^2 + 2c = 0$ and the same phase portraits as the system

$$\begin{cases} \frac{d\varphi}{d\zeta} = y(\varphi^2 - y^2 + 2c), \\ \frac{dy}{d\zeta} = \varphi(\varphi^2 - y^2 + 2(a + c)), \end{cases} \tag{33}$$

where $d\xi = (\varphi^2 - y^2 + 2c)d\zeta$, for $\varphi^2 - y^2 + 2c \neq 0$.

If $c = -2a$ $(a > 0)$ and $h = h_0 = 4c^2$, we have the following algebraic equation of homoclinic orbit:

$$y^2 = \varphi^2 - 4a + 2\sqrt{4a^2 - a\varphi^2}, \tag{34}$$

which is tangent to the hyperbola $\varphi^2 - y^2 + 2c = 0$ at point $(\pm 2\sqrt{a}, 0)$ (see Figure 3(a)). Let $\varphi(0) = 2\sqrt{a}$, then from (34) and the first equation of (31), we obtain

$$\int_{2\sqrt{a}}^{\varphi} \frac{d\varphi}{\sqrt{\varphi^2 - 4a + 2\sqrt{4a^2 - a\varphi^2}}} = \pm\xi. \tag{35}$$

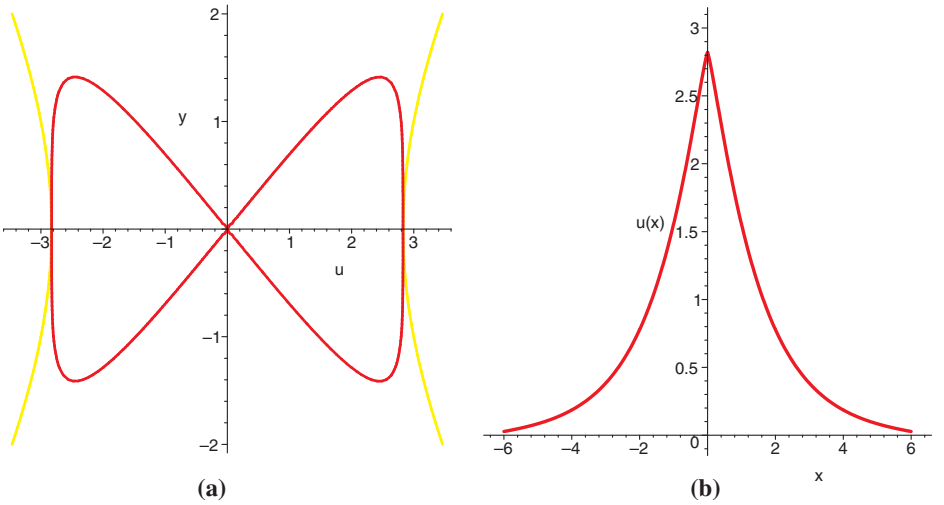

Figure 3. (a) The homoclinic orbit $H(\varphi, y) = 0$ defined by (32). (b) The profile of pseudo-cuspon.

Letting $\psi^2 = 4a^2 - a\phi^2$ leads Equation (35) to

$$\int_0^{\psi} \frac{\psi d\psi}{(2a - \psi)\sqrt{(2a + \psi)\psi}} = \pm\sqrt{a}\xi. \tag{36}$$

Therefore, we obtain the following parametric solutions of (10):

$$\begin{cases} \phi(\xi) = \pm\sqrt{\frac{c^2 - \psi^2(\xi)}{a}}, \\ I_3(\psi) + \frac{\sqrt{2}}{2} I_4[\psi] = \pm\sqrt{a}\xi, \end{cases} \tag{37}$$

where

$$I_3(\psi) = \ln\left|\frac{a}{a + \psi + \sqrt{\psi(\psi + 2a)}}\right|, \tag{38}$$

$$I_4(\psi) = \ln\left|\frac{a^2(2a + 3\psi + 2\sqrt{2\psi(\psi + 2a)})}{2a - \psi}\right|. \tag{39}$$

According to Equations (34) and (30), the parametric solution should satisfy

$$\left(\frac{d\varphi}{d\xi}\right)^2 = \varphi^2 - 4a + 2\sqrt{a(4a - \varphi^2)} \tag{40}$$

and

$$\left(\frac{d^2\varphi}{d\xi^2}\right)^2 = \frac{\varphi^2(a-\sqrt{a(4a-\varphi^2)})^2}{a(4a-\varphi^2)}. \tag{41}$$

Therefore, when $\xi \to 0$, then $\varphi \to \pm 2\sqrt{a}$, $\frac{d\varphi}{d\xi} \to 0$, $\frac{d^2\varphi}{d\xi^2} \to \pm\infty$. Thus, the second-order derivative of the parametric solution has an infinity jump at its crest $\xi = 0$. Hence, the parametric solution (37) is a pseudo-cuspon solution to Equation (10). The profile of the pseudo-cuspon wave is shown in Figure 3(b).

3. Hyperbolic singular curves and singular traveling waves

The traveling wave system (3) for Equations (10)–(12) admits hyperbolic singular curves in the phase plane. In the following, let us focus on the traveling wave solution of Equation (10).

The singular point distribution of system (33) is given below.

(1) For $c < 0$, when $a + c \geq 0$, the system (33) has only one equilibrium point $O(0, 0)$; when $a + c < 0$, the system (33) has three equilibrium points $O(0, 0)$ and $P_{\pm}(\pm\varphi_1, 0)$, where $\varphi_1 = \sqrt{-2(a+c)}$.
(2) For $c > 0$, when $a + c \geq 0$, the system (33) has three equilibrium points $O(0, 0)$ and $S_{\pm}(0, \pm\sqrt{2c})$; when $a + c < 0$, the system (33) has five equilibrium points $O(0, 0)$, $P_{\pm}(\pm\varphi_1, 0)$ and $S_{\pm}(0, \pm\sqrt{2c})$.

In addition, from Equation (32), we have

$$\begin{aligned} h_0 &= H(0, 0) = 4c^2, \\ h_1 &= H(\pm\varphi_1, 0) = 8a(a-c), \\ h_c &= H(\pm\sqrt{-2c}, 0) = -8ac. \end{aligned} \tag{42}$$

It is known that a solitary wave solution of Equation (10) corresponds to a homoclinic orbit of the system (31). Obviously, as $c < 0, a > 0, a + c < 0$, there exists a homoclinic orbit defined by $H(\varphi, y) = h_0$.

PROPOSITION 1. *Suppose that $a > 0, c < 0$, then we have the following results:*

(1) For $-a < c < 0$, there is a family of periodic orbits enclosing the center point $(0, 0)$. If $h = h_c$, the periodic orbit defined by $H(\varphi, y) = h_c$ is tangent to the hyperbola $\varphi^2 - y^2 + 2c = 0$ at point $(\pm\sqrt{-2c}, 0)$.
(2) For $-2a < c < -a$, there are two families of periodic orbits enclosing the center points $(\varphi_1, 0)$ and $(-\varphi_1, 0)$ and surrounded by a homoclinic orbit $H(\varphi, y) = h_0$ containing the saddle point $(0, 0)$. The homoclinic orbit does not intersect with the singular curve $\varphi^2 - y^2 + 2c = 0$.

If $h \in (h_0, h_c)$, there is a family of periodic orbits defined by $H(\varphi, y) = h$ outside the homoclinic orbit. If $h = h_c$, the periodic orbit defined by $H(\varphi, y) = h_c$ is tangent to the hyperbola $\varphi^2 - y^2 + 2c = 0$ at point $(\pm\sqrt{-2c}, 0)$.

(3) For $c = -2a$, there are two families of periodic orbits enclosing the center points $(\varphi_1, 0)$ and $(-\varphi_1, 0)$ and surrounded by a homoclinic orbit $H(\varphi, y) = h_0$ containing the saddle point $(0, 0)$. The homoclinic orbit is tangent to the singular curve $\varphi^2 - y^2 + 2c = 0$.

(4) For $c < -2a$, the homoclinic orbit defined by $H(\varphi, y) = h_0$ intersects with the singular curve $\varphi^2 - y^2 + 2c = 0$.

The phase portraits of the system (33) are shown in Figure 4 for $a > 0, c < 0$. Let us discuss the above four cases in detail below.

(1) Case I: $-a < c < 0$.

If $h \in (h_0, h_c)$, the periodic orbit defined by $H(\varphi, y) = h$ has no intersection point with the hyperbola $\varphi^2 - y^2 + 2c = 0$. Thus, Equation (10) has a family of smooth periodic wave solutions. The algebraic equation of periodic orbit is given by

$$y^2 = \varphi^2 + 2c + \sqrt{h - 4a\varphi^2}, \tag{43}$$

which intersects with the φ-axis at two points $(-\varphi_m, 0)$ and $(\varphi_m, 0)$. From Equation (43) and the first equation of (31), one may compute the parametric representation for the periodic orbit below

$$\int_{\varphi}^{\varphi_m} \frac{d\varphi}{\sqrt{\varphi^2 + 2c + \sqrt{h - 4a\varphi^2}}} = |\xi - 2nT_1|, \tag{44}$$

where $|\xi - 2nT_1| \leq T_1$ and

$$T_1 = \int_{\varphi}^{\varphi_m} \frac{d\varphi}{\sqrt{\varphi^2 + 2c + \sqrt{h - 4a\varphi^2}}}. \tag{45}$$

Letting $\psi^2 = h - 4a\varphi^2$ in Equation (43) yields $y^2 = \frac{1}{4a}(\psi_M - \psi)(\psi - \psi_m)$, where $\psi_M = 2a + \sqrt{4a^2 + 8ac + h}$ and $\psi_m = 2a - \sqrt{4a^2 + 8ac + h}$. By the first equation of the system (31), we have

$$\int_{\psi_m}^{\psi} \frac{\psi d\psi}{\sqrt{(\psi_M - \psi)(\psi - \psi_m)(h - \psi^2)}} = \pm\xi. \tag{46}$$

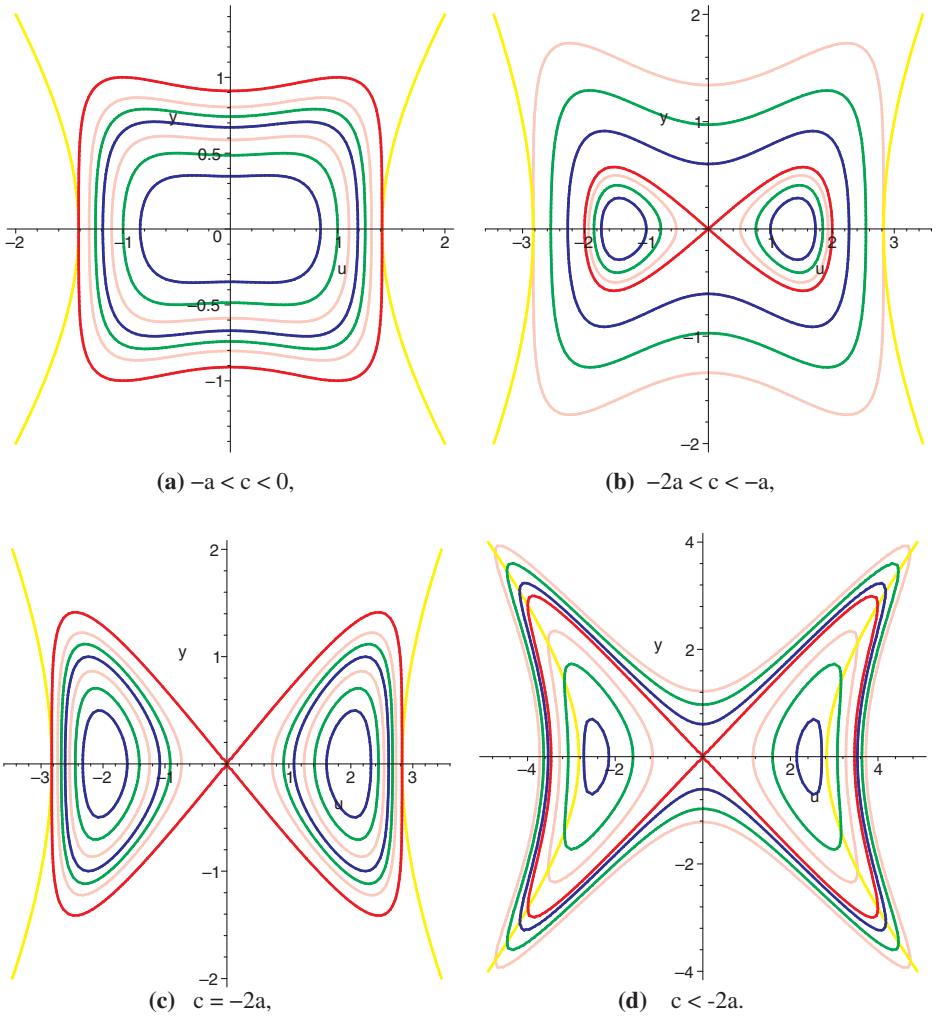

(a) −a < c < 0, **(b)** −2a < c < −a, **(c)** c = −2a, **(d)** c < -2a.

Figure 4. The phase portraits of the system (33) for $c < 0, a > 0$.

Therefore, we obtain the following parametric representations of smooth periodic wave solutions to Equation (10):

$$\begin{aligned}
\varphi(\tau) &= \pm\sqrt{\tfrac{h-\psi^2(\tau)}{4a}},\\
\psi(\tau) &= \tfrac{2\sqrt{h}(\psi_M-\psi_m)-\psi_M(\sqrt{h}-\psi_m)sn^2(\tau,k)}{\psi_M-\psi_m-(\sqrt{h}-\psi_m)sn^2(\tau,k)},\\
\xi(\tau) &= \tfrac{1}{\alpha^2\sqrt{(\psi_M-\psi_m)}}[(\alpha^2-\alpha_1^2)\Pi(\arcsin(sn(\tau,k)),\alpha^2,k)+\alpha_1^2\tau],
\end{aligned} \tag{47}$$

where

$$\alpha^2 = \frac{\sqrt{h} - \psi_m}{\psi_M - \psi_m},\ \alpha_1^2 = \frac{\psi_M(\sqrt{h} - \psi_m)}{\sqrt{h}(\psi_M - \psi_m)},\ k^2 = \frac{(\sqrt{h} - \psi_m)(\psi_M + \sqrt{h})}{2\sqrt{h}(\psi_M - \psi_m)}, \quad (48)$$

and $sn(\tau, k)$ is the Jacobian elliptic function with the modulus k and Π is the elliptic integral of the third kind.

If $h = -8ac$, the periodic orbit is tangent to the hyperbola $\varphi^2 - y^2 + 2c = 0$ at point $(\pm\sqrt{-2c}, 0)$. The corresponding periodic wave solution satisfies

$$\left(\frac{d\varphi}{d\xi}\right)^2 = \varphi^2 + 2c + \sqrt{-4a(2c + \varphi^2)} \quad (49)$$

and

$$\left(\frac{d^2\varphi}{d\xi^2}\right)^2 = -\frac{\varphi^2\left(2a - \sqrt{-4a(\varphi^2 + 2c)}\right)^2}{4a(\varphi^2 + 2c)}. \quad (50)$$

Along this orbit when $\varphi \to \pm\sqrt{-2c}$, then $\frac{d\varphi}{d\xi} \to 0$, $\frac{d^2\varphi}{d\xi^2} \to \pm\infty$. Thus, when $h \to \pm\sqrt{-2c}$, the smooth periodic wave evolves into a singular periodic wave (see Figure 5).

The singular periodic wave can be written as

$$\int_{\varphi}^{\sqrt{-2c}} \frac{d\varphi}{\sqrt{\varphi^2 + 2c + \sqrt{-4a(\varphi^2 + 2c)}}} = |\xi - 2nT_2|, \quad (51)$$

where $|\xi - 2nT_2| \le T_2$ and

$$T_2 = \int_{-\sqrt{-2c}}^{\sqrt{-2c}} \frac{d\varphi}{\sqrt{\varphi^2 + 2c + \sqrt{-4a(\varphi^2 + 2c)}}}. \quad (52)$$

Letting $\psi^2 = -4a(\varphi^2 + 2c)$ in Equation (32) leads to $y^2 = \frac{1}{4a}(4a - \psi)\psi$. By the first equation of the system (31), we have

$$\int_0^{\psi} \frac{\psi d\psi}{\sqrt{\psi(4a - \psi)(-8ac - \psi^2)}} = \pm\xi. \quad (53)$$

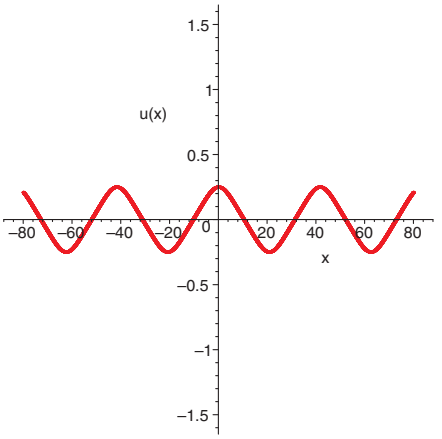

(a) $h = 4.0039$

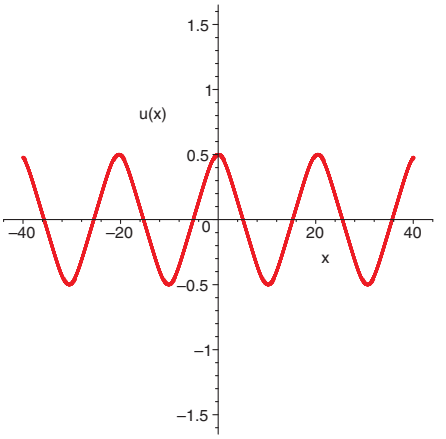

(b) $h = 4.0635$

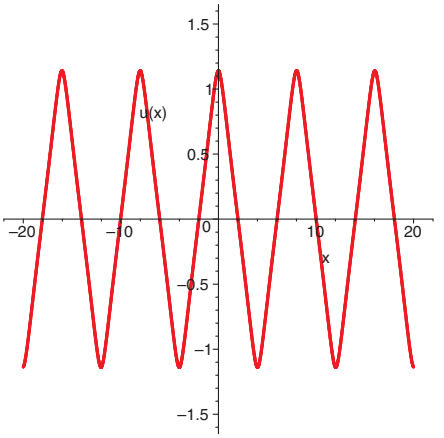

(c) $h = 8$

Figure 5. When $-a < c < 0$, as h from h_0 tends to h_c, the smooth periodic waves evolve into a singular periodic wave.

Therefore, we obtain the following parametric representations of singular periodic wave solutions to Equation (10):

$$\begin{aligned}
\varphi(\tau) &= \pm\sqrt{\tfrac{-8ac-\psi^2(\tau)}{4a}},\\
\psi(\tau) &= \tfrac{4a\sqrt{-2ac}cn^2(\tau,k)}{2a-\sqrt{-2ac}sn^2(\tau,k)},\\
\xi(\tau) &= \tfrac{\sqrt{-2ac}}{\alpha^2\sqrt{a\sqrt{-2ac}}}[\alpha^2\Pi(\arcsin(sn(\tau,k)),\alpha^2,k)+\tau],
\end{aligned} \tag{54}$$

where

$$\alpha^2 = \frac{\sqrt{-2ac}}{2a}, \qquad k^2 = \frac{2a + \sqrt{-2ac}}{4a}. \tag{55}$$

(2) Case II: $-2a < c < -a$.

If $h \in (h_1, h_0)$, the periodic orbit defined by $H(\varphi, y) = h$ has no intersection point with the hyperbola $\varphi^2 - y^2 + 2c = 0$. Thus, Equation (10) has a family of smooth periodic wave solutions. The periodic orbit intersects with the φ-axis at two points $(\varphi_m, 0)$ and $(\varphi_M, 0)$. From Equation (32) and the first equation of (31), we have the following parametric representation for the periodic orbit:

$$\int_{\varphi}^{\varphi_M} \frac{d\varphi}{\sqrt{\varphi^2 + 2c + \sqrt{h - 4a\varphi^2}}} = |\xi - 2nT_3|, \tag{56}$$

where $|\xi - 2nT_3| \le T_3$ and

$$T_3 = \int_{\varphi_m}^{\varphi_M} \frac{d\varphi}{\sqrt{\varphi^2 + 2c + \sqrt{h - 4a\varphi^2}}}. \tag{57}$$

Letting $\psi^2 = h - 4a\varphi^2$ in Equation (43) yields $y^2 = \frac{1}{4a}(\psi_M - \psi)(\psi - \psi_m)$, where $\psi_M = 2a + \sqrt{4a^2 + 8ac + h}$ and $\psi_m = 2a - \sqrt{4a^2 + 8ac + h}$. By the first equation of the system (31), we have

$$\int_{\psi_m}^{\psi} \frac{\psi d\psi}{\sqrt{(\psi_M - \psi)(\psi - \psi_m)(h - \psi^2)}} = \pm\xi. \tag{58}$$

Therefore, we obtain the following parametric representations of smooth periodic wave solutions to Equation (10):

$$\begin{aligned}
&\varphi(\tau) = \pm\sqrt{\tfrac{h - \psi^2(\tau)}{4a}},\\
&\psi(\tau) = \tfrac{(\sqrt{h} - \psi_m)\psi_M - \sqrt{h}(\psi_M - \psi_m)sn^2(\tau, k)}{\sqrt{h} - \psi_m - (\psi_M - \psi_m)sn^2(\tau, k)},\\
&\xi(\tau) = \tfrac{2\psi_M}{\alpha^2\sqrt{(\sqrt{h} - \psi_m)(\psi_M + \sqrt{h})}}[(\alpha^2 - \alpha_1^2)\Pi(\arcsin(sn(\tau, k)), \alpha^2, k) + \alpha_1^2\tau],
\end{aligned} \tag{59}$$

where

$$\alpha^2 = \frac{\psi_M - \psi_m}{\sqrt{h} - \psi_m}, \quad \alpha_1^2 = \frac{\sqrt{h}(\psi_M - \psi_m)}{\psi_M(\sqrt{h} - \psi_m)}, \quad k^2 = \frac{2\sqrt{h}(\psi_M - \psi_m)}{(\sqrt{h} - \psi_m)(\sqrt{h} + \psi_M)}. \tag{60}$$

If $h = h_0$, the homoclinic orbit defined by $H(\varphi, y) = h_0$ has no intersection point with the hyperbola $\phi^2 - y^2 + 2c = 0$. Thus, Equation (10) has a smooth

solitary wave solution. To find a parametric representation of solitary wave solution, let us start from the algebraic equation of homoclinic orbit

$$y^2 = \varphi^2 + 2c \pm 2\sqrt{c^2 - a\varphi^2}. \tag{61}$$

The sign before the term $2\sqrt{c^2 - a\varphi^2}$ is dependent on the interval of φ. Under the condition $-2a < c < -a$ and for $\varphi \in (-2\sqrt{-(a+c)}, 2\sqrt{-(a+c)})$, we need to take $+$ before the term $2\sqrt{c^2 - a\varphi^2}$. From Equation (61) and the first equation of (31), we have the following parametric representation for the corresponding homoclinic orbits:

$$\int_{2\sqrt{-(a+c)}}^{\varphi} \frac{d\varphi}{\sqrt{\varphi^2 + 2c + 2\sqrt{c^2 - a\varphi^2}}} = \pm\xi. \tag{62}$$

Letting $\psi^2 = c^2 - a\varphi^2$ in Equation (61) leads to $y^2 = \frac{1}{a}(\psi - \psi_1)(\psi_2 - \psi)$, where $\psi_1 = -c$, $\psi_2 = 2a + c$. By the first equation of the system (31), we obtain

$$\int_{\psi_2}^{\psi} \frac{\psi d\psi}{(\psi + c)\sqrt{(\psi - \psi_2)(\psi - c)}} = \pm\sqrt{a}\xi. \tag{63}$$

Therefore, we arrive at the following parametric representations of smooth solitary wave solutions to Equation (10):

$$\begin{cases} \phi(\xi) = \pm\sqrt{\frac{c^2 - \psi^2(\xi)}{a}}, \\ I_5(\psi) + \frac{\sqrt{2}c}{2\sqrt{2c(a+c)}} I_6[\psi] = \pm\sqrt{a}\xi, \end{cases} \tag{64}$$

where

$$I_5(\psi) = \ln\left|\frac{\psi - (a+c) + \sqrt{(2a + c - \psi)(c - \psi)}}{a(\psi + c)}\right|, \tag{65}$$

$$I_6(\psi) = \ln\left|\frac{-c(3a+c) - (a+2c)\psi + 2\sqrt{c(a+c)(2a+c-\psi)(c-\psi)}}{a(\psi + c)}\right|. \tag{66}$$

If $h \in (h_0, h_c)$, the periodic orbit defined by $H(\varphi, y) = h$ has no intersection point with the hyperbola $\varphi^2 - y^2 + 2c = 0$. Thus, Equation (10) has a family of periodic wave solutions with the same parametric representation as (47).

If $h = -8ac$, the periodic orbit is tangent to the hyperbola $\varphi^2 - y^2 + 2c = 0$ at the point $(\pm\sqrt{-2c}, 0)$. Thus, when $h \to \pm\sqrt{-2c}$, the smooth periodic wave evolves into a singular periodic wave with the same parametric representation as (54).

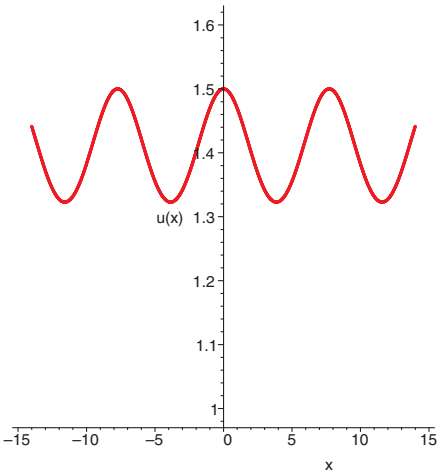

(a) $h = 60.0625$

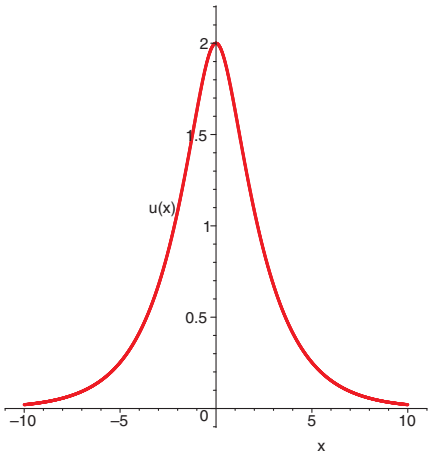

(b) $h = 64$

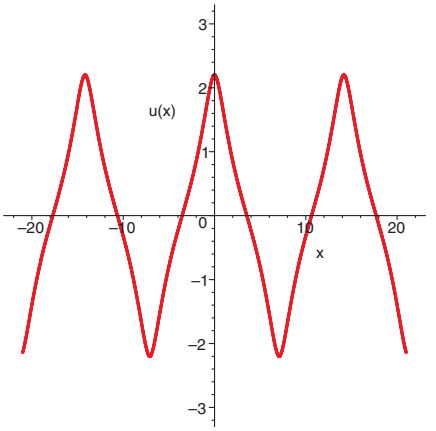

(c) $h = 68.0656$

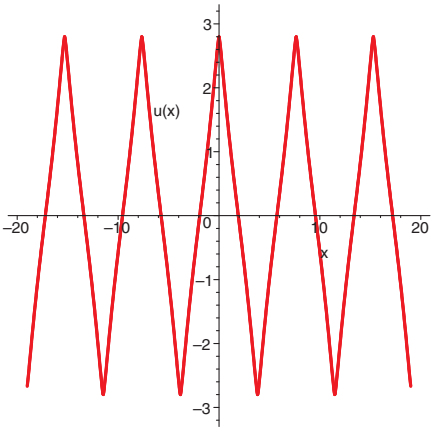

(d) $h = 96$

Figure 6. When $-2a < c < -a$, as h from h_1 tends to h_0, the smooth periodic waves evolve into a smooth solitary wave; as h from h_0 tends to h_c, the smooth solitary waves evolve into a singular periodic wave.

Based on the above analysis, when $-2a < c < -a$, as long as $h \in (h_1, h_0)$ and $h \to h_0$, the smooth periodic waves evolve into a smooth solitary wave; as long as $h \in (h_0, h_c)$ and $h \to h_c$, the smooth solitary waves evolve into a singular periodic wave. That procedure can be simulated by Maple and shown in Figures 6(a)–(d).

(3) Case III: $c = -2a$.

If $h \in (h_1, h_0)$, then the periodic orbit defined by $H(\varphi, y) = h$ has no intersection point with the hyperbola $\varphi^2 - y^2 + 2c = 0$. Thus, Equation (10)

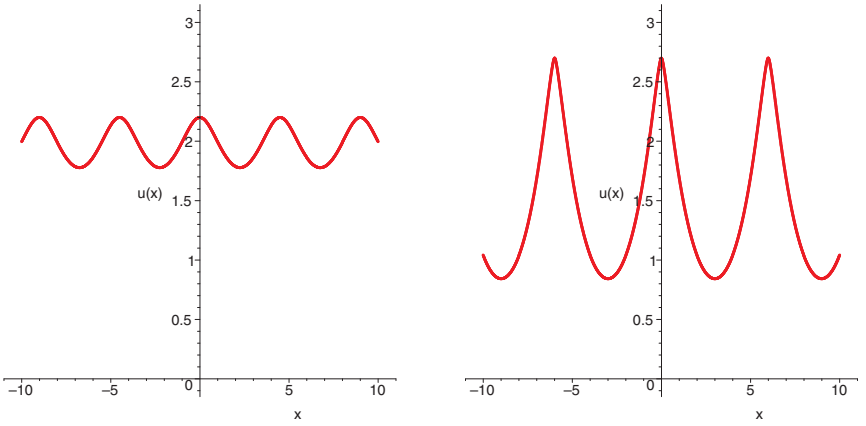

(a) $h = 48.7056$ **(b)** $h = 58.8241$

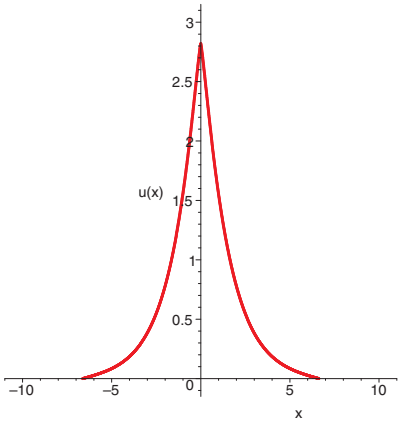

(c) $h = 64$

Figure 7. When $c = -2a$, as h from h_1 tends to h_0, the smooth periodic waves evolve into a singular solitary wave.

has a family of smooth periodic wave solutions with the same parametric representation as (59).

If $h = h_0$, the homoclinic orbit is tangent to the hyperbola $\varphi^2 - y^2 + 2c = 0$ at point $(\pm 2\sqrt{a}, 0)$. The homoclinic orbit corresponds to a pseudo-cuspon given in Section 2. When $h \to \pm\sqrt{-2c}$, the smooth periodic wave evolves into a pseudo-cuspon. That procedure can be simulated by Maple and shown in Figures 7(a)–(c).

(4) Case IV: $c < -2a$.

To understand the presence of M-/W-shape solitary wave solutions, let us make a further study about the case of $c < -2a$. In this case, the hyperbola $\varphi^2 - y^2 + 2c = 0$ intersects with the homoclinic orbit $H(\varphi, y) = h_0$ at four

points $Q_1^{\pm}(-\varphi^*, \pm y^*)$ and $Q_2^{\pm}(\varphi^*, \pm y^*)$, where $\varphi^* = -\frac{c\sqrt{a}}{a}$, $y^* = \sqrt{\frac{c(2a+c)}{a}}$. We know $y^2 = \varphi^2 + 2c + 2\sqrt{c^2 - a\varphi^2}$ in the interval between negative and positive half branch of the hyperbola $\varphi^2 - y^2 + 2c = 0$. However, on the left-hand side of negative half branch and right-hand side of positive half branch of the hyperbola $\varphi^2 - y^2 + 2c = 0$, we have $y^2 = \varphi^2 + 2c - 2\sqrt{c^2 - a\varphi^2}$. Therefore, we can, respectively, write them as follows:

$$y^2 = \frac{1}{a}(2a + c - \psi)(\psi + c), |\psi| \geq \sqrt{c^2 + 2ac - ay^2}, \tag{67}$$

and

$$y^2 = \frac{1}{a}(2a + c + \psi)(c - \psi), |\psi| < \sqrt{c^2 + 2ac - ay^2}, \tag{68}$$

where $\psi^2 = c^2 - a\varphi^2$.

Next we define a value ξ_0 by satisfying $\varphi(\xi_0) = -\frac{c\sqrt{a}}{a}$. Let us partition the whole real axis R into $(-\infty, -\xi_0) \cup (\xi_0, +\infty)$ and $(-\xi_0, \xi_0)$. Using Equations (31), (67), and (68), we arrive at the following M-shape solitary wave solutions:

$$\begin{cases} \varphi(\xi) = \sqrt{\frac{c^2 - \psi^2(\xi)}{a}}, \\ I_7(\psi) - I_7[-(2a + c)] = \pm\xi, \quad \xi \in (-\xi_0, \xi_0), \\ I_8(\psi) - I_8(0) = \pm(\xi_0 - \xi), \quad \xi \in (-\infty, -\xi_0) \cup (\xi_0, +\infty), \end{cases} \tag{69}$$

where

$$I_7(\psi) = J_1(\psi) - \frac{c}{\sqrt{c^2 + ac}} J_2(\psi),$$

$$J_1(\psi) = \ln|\psi + a + c + \sqrt{\psi^2 + 2(a + c)\psi + 2ac + c^2}|,$$

$$J_2(\psi) = \ln\left|\frac{4c^2 + 6ac + 2(a + 2c)\psi + 4\sqrt{(c^2 + ac)(\psi^2 + 2(a + c)\psi + 2ac + c^2)}}{\psi - c}\right|,$$

$$I_8(\psi) = J_3(\psi) + \frac{c}{\sqrt{c^2 + ac}} J_4(\psi),$$

$$J_3(\psi) = \ln|\psi - a - c + \sqrt{\psi^2 - 2(a + c)\psi + 2ac + c^2}|,$$

$$J_4(\psi) = \ln\left|\frac{4c^2 + 6ac - 2(a + 2c)\psi + 4\sqrt{(c^2 + ac)(\psi^2 - 2(a + c)\psi + 2ac + c^2)}}{\psi + c}\right|.$$

The profile of M-shape solitary wave is shown in Figure 8(c). The M-shape soliton (69) is the same kind of solution as the one in Refs. [31, 43].

Remark 1. It is worth pointing out that unlike the case of having a straight line as a singular curve in the system (3), the singular curve (now

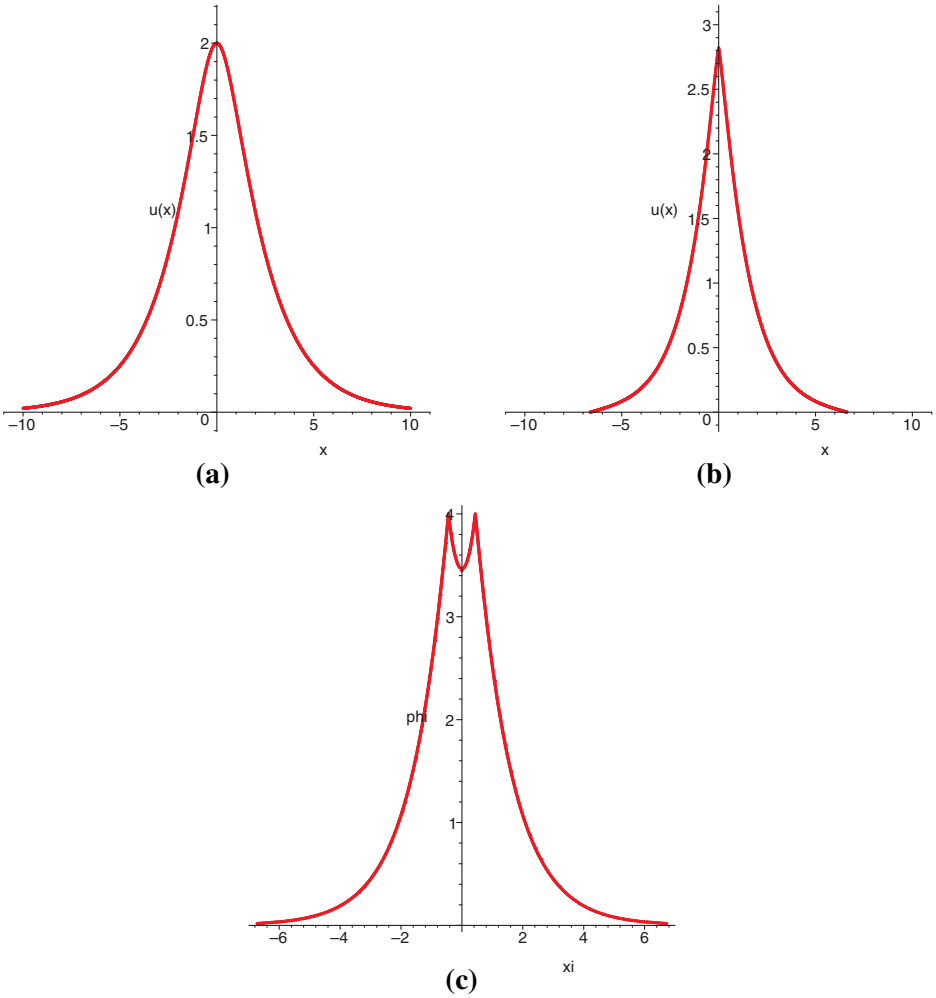

Figure 8. (a) Smooth solitary wave, (b) singular solitary wave, (c) M-shape solitary waves.

hyperbola) $\varphi^2 - y^2 + 2c = 0$ is not a solution of the system (31). The hyperbola $\varphi^2 - y^2 + 2c = 0$ intersects with the homoclinic orbit $H(\varphi, y) = 0$ at four points $Q_1^{\pm}(-\varphi^*, \pm y^*)$ and $Q_2^{\pm}(\varphi^*, \pm y^*)$, and the homoclinic orbit $H(\varphi, y) = 0$ intersects with the φ-axis at three points $O(0, 0)$ and $Q_3^{\pm}(\pm 2\sqrt{-(a + c)}, 0)$ (see Figure 4(d)). This hyperbola is the infinite isocline of the vector field for the system (33). Differing from the system (31), the hyperbola $\varphi^2 - y^2 + 2c = 0$ of the system (33) is a singular curve of the vector fields of the system. Here, we discuss the case of $c < -2a < 0$. Clearly, on both the left- and the right-hand branches of the hyperbola $\varphi^2 - y^2 + 2c = 0$, when ξ varies along the loop orbit defined by $H(\varphi, y) = h_0$, the vector fields of the system (31)

have a different direction. In fact, on the segment OQ_2^+, $\frac{d\varphi}{d\xi} > 0$, $\frac{dy}{d\xi} > 0$; on the segment OQ_2^-, $\frac{d\varphi}{d\xi} < 0$, $\frac{dy}{d\xi} > 0$; on the segment $Q_2^-Q_3^+$, $\frac{d\varphi}{d\xi} < 0$, $\frac{dy}{d\xi} > 0$; and on the segment $Q_3^+Q_2^+$, $\frac{d\varphi}{d\xi} > 0$, $\frac{dy}{d\xi} > 0$. Those imply that the loop orbit of the system (31), defined by $H(\varphi, y) = h_0$, consists of three breaking solutions [33].

4. Elliptic singular curves and singular traveling waves

In this section, we consider the nonlinear wave equations associated with an elliptic singular curve. Let us take the FOR equation (13) as our example. Changing variable from $u(\xi)$ to $\varphi(\xi)$ and taking integration with respect to ξ leads to an ordinary differential equation

$$\frac{d^2\varphi}{d\xi^2} = -\frac{2g + 2(a+c)\varphi + \varphi^3 + \varphi(\frac{d\varphi}{d\xi})^2}{2c + \varphi^2 + (\frac{d\varphi}{d\xi})^2},\ g = \text{constant}, \tag{70}$$

which is equivalent to the following planar system:

$$\begin{cases} \frac{d\varphi}{d\xi} = y, \\ \frac{dy}{d\xi} = -\frac{2g+2(a+c)\varphi+\varphi^3+\varphi y^2}{\varphi^2+y^2+2c}, \end{cases} \tag{71}$$

with the first integral below

$$H(\varphi, y) = \frac{1}{4}(\varphi^2 + y^2 + 2c)^2 + a\varphi^2 + 2g\varphi. \tag{72}$$

The system (71) is not Hamiltonian yet. However, if we define a new independent variable ζ through the differential equation $d\xi = (\varphi^2 + \phi^2 + 2c)d\zeta$, then we may obtain the Hamiltonian form as follows:

$$\begin{cases} \frac{d\varphi}{d\zeta} = y(\varphi^2 + y^2 + 2c), \\ \frac{dy}{d\zeta} = -(2g + 2(a+c)\varphi + \varphi^3 + \varphi y^2), \end{cases} \tag{73}$$

with Hamiltonian function (72). The system (73) has the same phase portraits as the system (71) except for the singular elliptic curve $\varphi^2 + y^2 + 2c = 0$.

The system (73) possesses very complex dynamical behaviors [41]. If $g^2 < -2ca^2$, there are two symmetrical singular points $S(\varphi_e, \pm y_e)$, where $\varphi_e = -\frac{g}{a}$ and $y_e = \sqrt{-\frac{g^2}{a^2} - 2c}$. If $g^2 < -\frac{32}{27}(a+c)^3$, there are three singular points $P_i(\varphi_i, 0), (i = 1, 2, 3)$ on the φ-axis, where $\varphi_1 < \varphi_2 < \varphi_3$ are three roots of the cubic equation $\varphi^3 + 2(a+c)\varphi + 2g = 0$. Denote $h_i = H(\varphi_i, 0)$, $i = 1, 2, 3$, and let us discuss the following two cases.

Case I: $a > 0, c < 0, g^2 < -2a^2c$.

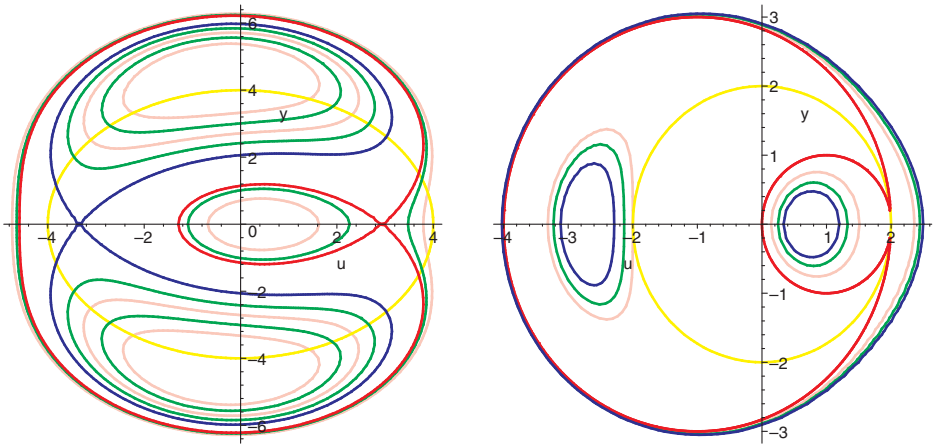

(a) $a > 0, c < 0, g < -a\sqrt{-2c}$ **(b)** $a > 0, c < 0, g = -a\sqrt{-2c}$

Figure 9. The phase portraits of the system (4.2).

If $h \in (h_3, h_2)$, the periodic orbit defined by $H(\varphi, y) = h$ has no intersection point with the singular curve $\varphi^2 + y^2 + 2c = 0$ (ellipse, see Figure 9(a)). Thus, the FOR Equation (13) has a family of smooth periodic wave solutions. The periodic orbit has the following algebraic equation:

$$y^2 = -\varphi^2 - 2c - 2\sqrt{h - a\varphi^2 - 2g\varphi}, \tag{74}$$

which intersects with the φ-axis at two points $(\varphi_m, 0)$ and $(\varphi_M, 0)$. From (74) and the first equation of (71), we obtain the following parametric representation for the periodic orbit:

$$\int_{\varphi_m}^{\varphi} \frac{d\varphi}{\sqrt{-\varphi^2 - 2c - 2\sqrt{h - a\varphi^2 - 2g\varphi}}} = |\xi - 2nT_4|, \tag{75}$$

where $|\xi - 2nT_4| \leq T_4$ and

$$T_4 = \int_{\varphi_m}^{\varphi_M} \frac{d\varphi}{\sqrt{-\varphi^2 - 2c - 2\sqrt{h - a\varphi^2 - 2g\varphi}}}. \tag{76}$$

If $h = h_3$, there is a homoclinic orbit inside the ellipse $\varphi^2 + y^2 + 2c = 0$. The algebraic equation of the homoclinic orbit reads as

$$y^2 = -\varphi^2 - 2c - 2\sqrt{h_3 - a\varphi^2 - 2g\varphi}. \tag{77}$$

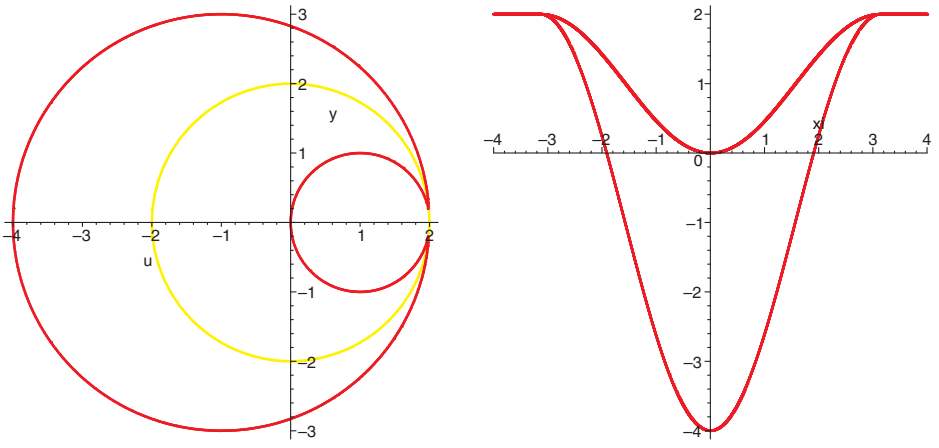

Figure 10. (a) The algebraic curve $H(\varphi, y) = 0$ defined by (4.3) for $a > 0, c < 0$, $g = -a\sqrt{-2c}$. (b) Profiles of two open upward compactons.

From (77) and the first equation of (71), we have the following parametric representation for the smooth solitary wave:

$$\int_{\varphi_m}^{\varphi} \frac{d\varphi}{\sqrt{-\varphi^2 - 2c - 2\sqrt{h_3 - a\varphi^2 - 2g\varphi}}} = \pm\xi. \tag{78}$$

Therefore, when $a > 0, c < 0, g < -a\sqrt{-2c}$, as h from h_2 tends to h_3, the smooth periodic waves evolve into a smooth solitary wave (see Figure11).

Case II: $a < 0, c < 0, g^2 = -2a^2c$.

In this case, the singular points of the system (73) are given by

$$E_1\left(-\frac{1}{2}(\sqrt{-8a - 2c} + \sqrt{-2c}), 0\right), E_2\left(\frac{1}{2}(\sqrt{-8a - 2c} - \sqrt{-2c}), 0\right), E_3(\sqrt{-2c}, 0).$$

In [42], we did a result on nilpotent singular points (see Ref. [46] for more details). Let $(0, 0)$ be an isolated point of the vector fields $(y + F(x, y), G(x, y))$, where F and G are analytic functions in a neighborhood of the origin required at least with quadratic terms in the variables x and y in their Taylor expansion. Let $y = f(x)$ be the solution of the equation $y + F(x, y) = 0$ in a neighborhood of $(0, 0)$. Assume that the development of the function $G(x, f(x))$ is of the form $Kx^k + HOT$, where K is a constant and HOT stands for higher order terms. If k is odd and $K > 0$, then the origin is a saddle point. Moreover, the saddle point has two separations tangent to the semi-axis $x < 0$, and the other two separations tangent to the semi-axis $x > 0$.

The eigenvalues of the Jacobian matrix M for the two singular points E_1 and E_2 are computed by two pairs of pure imaginary numbers $\lambda_1 = \pm\sqrt{A}i$

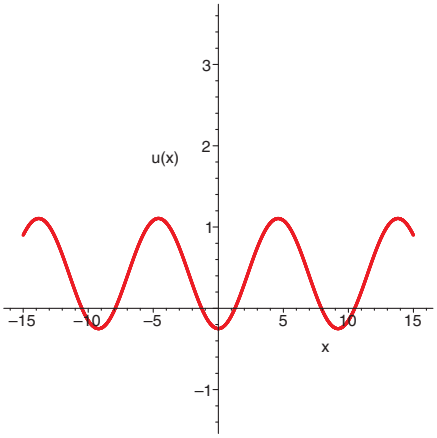

(a) $h = 98.68847656$

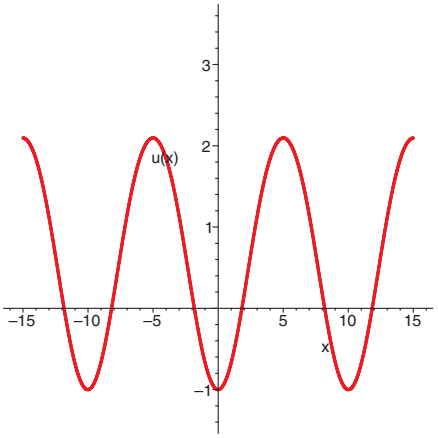

(b) $h = 91.25$

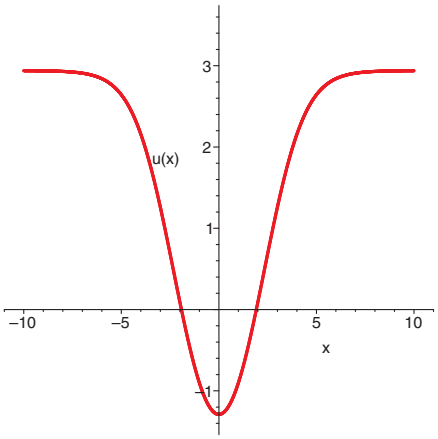

(c) $h = 87.21995056$

Figure 11. When $a > 0, c < 0, g < -a\sqrt{-2c}$, as h from h_2 tends to h_3, the smooth periodic waves evolve into a smooth solitary wave.

and $\lambda_2 = \pm\sqrt{B}i$, respectively, where

$$A = (\sqrt{4ac + c^2} - 2a + c)(3\sqrt{4ac + c^2} - 4a - c) \tag{79}$$

and

$$B = (\sqrt{4ac + c^2} + 2a - c)(4a + c - 3\sqrt{4ac + c^2}). \tag{80}$$

Thus, two singular points E_1 and E_2 are two centers.

For the singular point E_3, the Jacobian matrix is not zero and $detM = trM = 0$, therefore E_3 is a nilpotent point. Let $\varphi - \sqrt{-2c} \to \frac{\varphi}{4c-2a}$,

then the system (73) reads as

$$\begin{cases} \frac{d\varphi}{d\zeta} = G(\varphi, y), \\ \frac{dy}{d\zeta} = \varphi + F(\varphi, y), \end{cases} \tag{81}$$

where

$$G(\varphi, y) = \left(\frac{1}{4c - 2a}\varphi^2 + 2\sqrt{-2c}\varphi + y^2 \right) y \tag{82}$$

and

$$F(\varphi, y) = -\left(\frac{3\sqrt{-2c}}{(4c - 2a)^2}\varphi^2 + \frac{1}{(4c - 2a)^3}\varphi^3 + (\frac{1}{4c - 2a}\varphi + \sqrt{-2c})y^2 \right). \tag{83}$$

The equation $\varphi + F(\varphi, y) = 0$ implies $\varphi = \sqrt{-2c}y^2 + HOT$, thus we have

$$G(\varphi(y), y) = -2ay^3 + HOT, \tag{84}$$

which produces $K = -2a > 0$ and $k = 3$. Thus, E_3 is a nilpotent saddle point.

Let $h_c = H(-\sqrt{-2c}, 0)$. Then, if $h \in (h_1, h_c)$, the periodic orbit defined by $H(\varphi, y) = h$ has no intersection point with the singular curve (ellipse) $\varphi^2 + y^2 + 2c = 0$ (see Figure 9(b)). Thus, Equation (13) has a family of smooth periodic wave solutions. The algebraic equation of periodic orbit is given by

$$y^2 = -\varphi^2 - 2c + 2\sqrt{h - a\varphi^2 + 2a\sqrt{-2c}\varphi}, \tag{85}$$

which intersects with the φ-axis at two points $(\varphi_m, 0)$ and $(\varphi_M, 0)$. From (85) and the first equation of (71), we have the following parametric representation for the periodic orbit:

$$\int_{\varphi_m}^{\varphi} \frac{d\varphi}{\sqrt{-\varphi^2 - 2c + 2\sqrt{h - a\varphi^2 + 2a\sqrt{-2c}\varphi}}} = |\xi - 2nT_5|, \tag{86}$$

where $|\xi - 2nT_5| \leq T_5$ and

$$T_5 = \int_{\varphi_m}^{\varphi_M} \frac{d\varphi}{\sqrt{-\varphi^2 - 2c + 2\sqrt{h - a\varphi^2 + 2a\sqrt{-2c}\varphi}}}. \tag{87}$$

If $h = -6ac$, the periodic orbit is tangent to the singular curve (ellipse) $\varphi^2 + y^2 + 2c = 0$ at point $(-\sqrt{-2c}, 0)$. The corresponding periodic wave

solution satisfies

$$\left(\frac{d\varphi}{d\xi}\right)^2 = -\varphi^2 - 2c + 2\sqrt{-a(\varphi - 3\sqrt{-2c})(\varphi + \sqrt{-2c})} \tag{88}$$

and

$$\left(\frac{d^2\varphi}{d\xi^2}\right)^2 = \frac{(a\varphi - a\sqrt{-2c} + \varphi\sqrt{-a(\varphi - 3\sqrt{-2c})(\varphi + \sqrt{-2c})})^2}{-a(\varphi - 3\sqrt{-2c})(\varphi + \sqrt{-2c})}. \tag{89}$$

Therefore, along this orbit when $\varphi \to -\sqrt{-2c}$, one may have $\frac{d\varphi}{d\xi} \to 0$, $\frac{d^2\varphi}{d\xi^2} \to \pm\infty$. Thus, when $h \to -6ac$, the smooth periodic wave evolves into a singular periodic wave (see Figure 12).

The singular periodic wave can be expressed as

$$\int_{\varphi_m}^{\varphi} \frac{d\varphi}{\sqrt{-\varphi^2 - 2c + 2\sqrt{-a(\varphi - 3\sqrt{-2c})(\varphi + \sqrt{-2c})}}} = |\xi - 2nT_6|, \tag{90}$$

where $|\xi - 2nT_6| \le T_6$ and

$$T_6 = \int_{\varphi_m}^{-\sqrt{-2c}} \frac{d\varphi}{\sqrt{-\varphi^2 - 2c + 2\sqrt{-a(\varphi - 3\sqrt{-2c})(\varphi + \sqrt{-2c})}}}. \tag{91}$$

If $h \in (h_3, h_2)$, the periodic orbit defined by $H(\varphi, y) = h$ has no intersection point with the singular curve (ellipse) $\varphi^2 + y^2 + 2c = 0$. Thus, the FOR Equation (13) has a family of smooth periodic wave solutions. The algebraic equation of periodic orbit is given by

$$y^2 = -\varphi^2 - 2c + 2\sqrt{h - a\varphi^2 + 2a\sqrt{-2c}\varphi}, \tag{92}$$

which intersects with the φ-axis at two points $(\varphi_m, 0)$ and $(\varphi_M, 0)$. From (92) and the first equation of (71), we have the following parametric representation for the corresponding periodic orbit:

$$\int_{\varphi_m}^{\varphi} \frac{d\varphi}{\sqrt{-\varphi^2 - 2c + 2\sqrt{h - a\varphi^2 + 2a\sqrt{-2c}\varphi}}} = |\xi - 2nT_7|, \tag{93}$$

where $|\xi - 2nT_7| \le T_7$ and

$$T_7 = \int_{\varphi_m}^{\varphi_M} \frac{d\varphi}{\sqrt{-\varphi^2 - 2c + 2\sqrt{h - a\varphi^2 + 2a\sqrt{-2c}\varphi}}}. \tag{94}$$

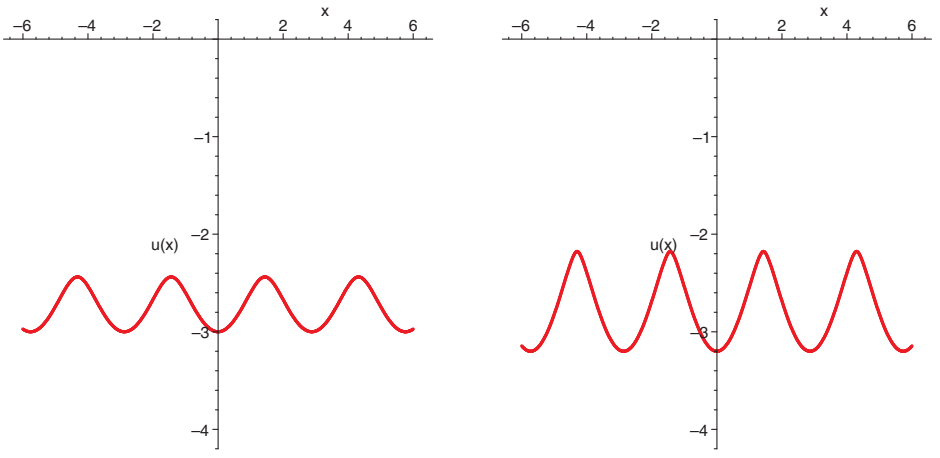

(a) $h = -14.75$ **(b)** $h = -13.3056$

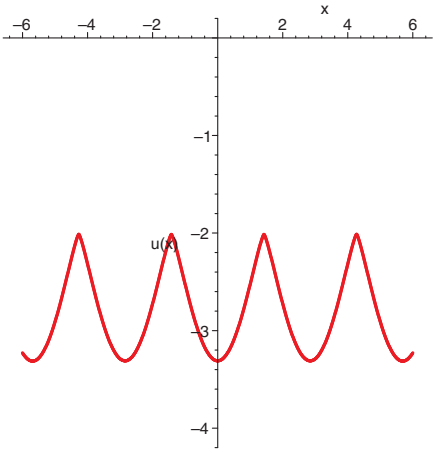

(c) $h = -12$

Figure 12. When $a > 0, c < 0, g = -a\sqrt{-2c}$, as h from h_1 tends to h_c, the smooth periodic waves evolve into a singular periodic wave.

If $h = h_3$, then there exist two close orbits

$$y^2 = -\varphi^2 - 2c \pm 2\sqrt{-a}(\varphi - \sqrt{-2c}), \tag{95}$$

which are tangent to the singular curve (ellipse) $\varphi^2 + y^2 + 2c = 0$ at the point E_3 (see Figure 10(a)). The two close orbits yield two new compactons (see

Figure 10(b))

$$\varphi(\xi) = \begin{cases} \sqrt{-a} - (\sqrt{-2c} - \sqrt{-a})\cos(\xi), & |\xi| \leq 2\pi, \\ \sqrt{-2c}, & \text{otherwise} \end{cases} \tag{96}$$

and

$$\varphi(\xi) = \begin{cases} -\sqrt{-a} - (\sqrt{-2c} + \sqrt{-a})\cos(\xi), & |\xi| \leq 2\pi, \\ \sqrt{-2c}, & \text{otherwise.} \end{cases} \tag{97}$$

Based on the above analysis, if $a > 0, c < 0, g = -a\sqrt{-2c}$, as long as h from h_2 tends to h_3, the smooth periodic waves evolve into a compacton. That procedure is just simulated by Maple and the graphs are shown in Figures 13(a)–(c).

5. Parabolic singular curves and singular traveling waves

In this section, we study the singular traveling waves of the DHS Equation (18). Its traveling wave system (3) admits parabolic singular curves in the phase plane.

To investigate the traveling wave solutions of the DHS Equation (18), substituting $u = u(x - ct) = \varphi(\xi)$ into (18), we have

$$-c\varphi''' = a\varphi' - 2\varphi'\varphi'' - \varphi\varphi''' + \frac{\lambda}{6}((\varphi')^3)''. \tag{98}$$

Integrating Equation (98) once and taking the integration constant as zero lead to

$$-c\varphi'' = a\varphi - \frac{1}{2}(\varphi')^2 - \varphi\varphi'' + \frac{\lambda}{6}((\varphi')^3)'. \tag{99}$$

Clearly, Equation (99) is equivalent to the following 2D system:

$$\begin{cases} \frac{d\varphi}{d\xi} = y, \\ \frac{dy}{d\xi} = \frac{a\varphi - \frac{1}{2}y^2}{\varphi - c - \frac{\lambda}{2}y^2}, \end{cases} \tag{100}$$

which has the first integral

$$H(\varphi, y) = 4y^2\varphi - 4a\varphi^2 - 4cy^2 - \lambda y^4 = h. \tag{101}$$

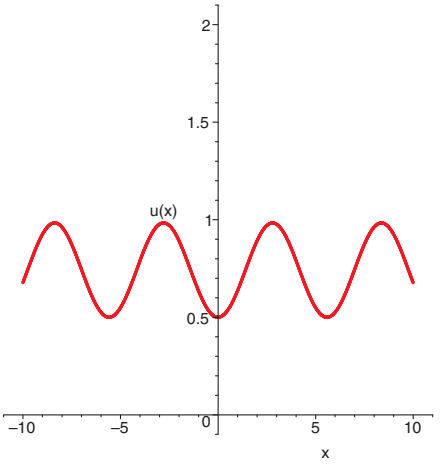

(a) $h = 5.265625$

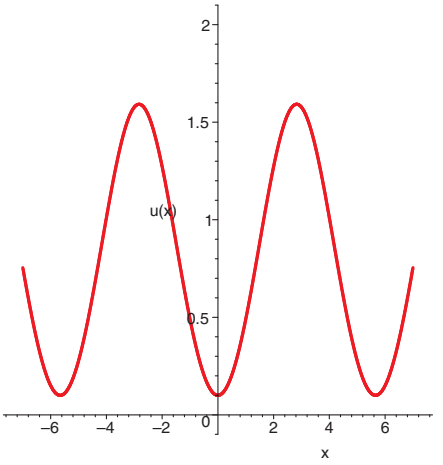

(b) $h = 4.370025$

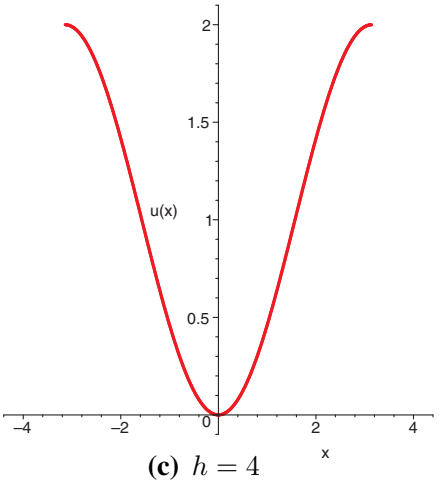

(c) $h = 4$

Figure 13. When $a > 0, c < 0, g = -a\sqrt{-2c}$, as h from h_2 tends to h_3, the smooth periodic waves evolve into a compacton.

The system (100) has a parabolic singular curve $\varphi - c - \frac{\lambda}{2}y^2 = 0$ and has the same phase portraits as the following system:

$$\begin{cases} \frac{d\varphi}{d\zeta} = y(\varphi - c - \frac{\lambda}{2}y^2), \\ \frac{dy}{d\zeta} = a\varphi - \frac{1}{2}y^2, \end{cases} \tag{102}$$

where $d\xi = (\varphi - c - \frac{\lambda}{2}y^2)d\zeta$, and $\varphi - c - \frac{\lambda}{2}y^2 \neq 0$. If $ac > 0$, then the origin is a center of the system (100). In addition, from Euation (101) we have

$$h_0 = H(0, 0) = 0, \quad h_c = H(c, 0) = -4ac^2. \tag{103}$$

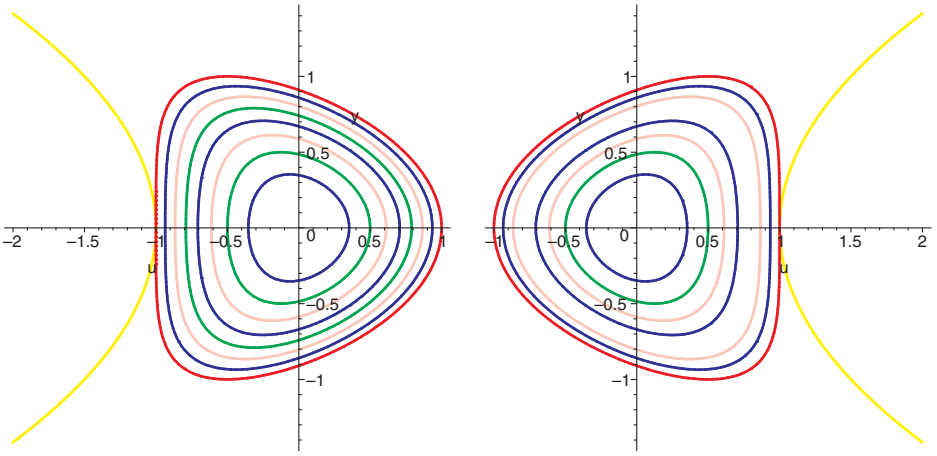

(a) $\lambda < 0, a < 0, c < 0$ **(b)** $\lambda > 0, a > 0, c > 0$

Figure 14. The phase portrait of the system (100) for $ac > 0$.

If $a < 0, c < 0, h \in (0, h_c)$, the periodic orbit defined by $H(\varphi, y) = h$ has no intersection point with the parabola $\varphi - c - \frac{\lambda}{2}y^2 = 0$ (see Figure 14(a)). Thus, the DHS Equation (18) has a family of smooth periodic wave solutions. The algebraic equation of periodic orbit is given by

$$y^2 = \frac{1}{2\lambda}(4\varphi - 4c \pm \sqrt{(4\varphi - 4c)^2 - 4\lambda(4a\varphi^2 + h)}), \tag{104}$$

where the sign before the term $\sqrt{(4\varphi - 4c)^2 - 4\lambda(4a\varphi^2 + h)}$ is dependent on the interval of φ. Under the condition $\lambda < 0, a < 0, c < 0$, for $\varphi \in (c, -c)$, we need to take minus sign. Therefore, the periodic orbit surrounding the center $O(0, 0)$ can be expressed as follows:

$$y = \pm\sqrt{\frac{1}{2\lambda}(4\varphi - 4c - \sqrt{(4\varphi - 4c)^2 - 4\lambda(4a\varphi^2 + h)})}, \quad (0 < h < -4ac^2), \tag{105}$$

which intersects with the φ-axis at two points $(\varphi_1^{\pm}.0) = \left(\pm\frac{1}{2}\sqrt{-\frac{h}{a}}, 0\right)$. From (105) and the first equation of (100), we have the following parametric representation for the periodic orbit:

$$\int_{\varphi}^{\varphi_1^+} \frac{d\varphi}{\sqrt{2c - 2\varphi + \sqrt{4(\varphi - c)^2 - \lambda(4a\varphi^2 + h)}}} = \frac{1}{\sqrt{-\lambda}}|\xi - 2nT_8|, \tag{106}$$

where $|\xi - 2nT_8| \leq T_8$ and

$$T_8 = \int_{\varphi_1^-}^{\varphi_1^+} \frac{\sqrt{-\lambda}d\varphi}{\sqrt{2c - 2\varphi + \sqrt{4(\varphi - c)^2 - \lambda(4a\varphi^2 + h)}}}. \tag{107}$$

If $h = -4ac^2$, the periodic orbit is tangent to the parabola $\varphi = \frac{\lambda}{2}y^2 + c$ at point $(c, 0)$. The corresponding periodic wave solution satisfies

$$\left(\frac{d\varphi}{d\xi}\right)^2 = \frac{1}{\lambda}(2\varphi - 2c - 2\sqrt{(\varphi - c)^2 - \lambda a(\varphi^2 - c^2)}) \tag{108}$$

and

$$\left(\frac{d^2\varphi}{d\xi^2}\right)^2 = \frac{(a\varphi - \frac{1}{\lambda}(\varphi - c - \sqrt{(\varphi - c)^2 - \lambda a(\varphi^2 - c^2)}))^2}{(\varphi - c)((1 - a\lambda)\varphi - (1 + a\lambda)c)}. \tag{109}$$

Subsequently, along this orbit when $\varphi \to c$, one may have $\frac{d\varphi}{d\xi} \to 0$, $\frac{d^2\varphi}{d\xi^2} \to \pm\infty$. Thus when $h \to -4ac^2$, the smooth periodic wave evolves into a singular periodic wave. That procedure may be simulated by Maple and shown in Figures 15(a)– (c).

The singular periodic wave can be expressed in the following form:

$$\int_{\varphi}^{\varphi_1^+} \frac{d\varphi}{\sqrt{2c - 2\varphi + 2\sqrt{(\varphi - c)^2 - \lambda a(\varphi^2 - c^2)}}} = \frac{1}{\sqrt{-\lambda}}|\xi - 2nT_9|, \tag{110}$$

where $|\xi - 2nT_9| \leq T_9$ and

$$T_9 = \int_{\varphi_1^-}^{\varphi_1^+} \frac{\sqrt{-\lambda}d\varphi}{\sqrt{2c - 2\varphi + 2\sqrt{(\varphi - c)^2 - \lambda a(\varphi^2 - c^2)}}}. \tag{111}$$

Particularly, when $a\lambda = 1$, letting $\psi^2 = 2c(c - \varphi)$ yields $y^2 = \frac{1}{\lambda c}(-\psi^2 - 2c\psi)$. By the first equation of the system (100), we have

$$\int_{\psi}^{-2c} \frac{\psi d\psi}{\sqrt{\psi(-2c - \psi)}} = \frac{\sqrt{c\lambda}}{\lambda}|\xi - 2nT_9|. \tag{112}$$

Therefore, we obtain the following parametric representations of singular periodic wave solutions for the DHS Equation (18):

$$\varphi(\xi) = c - \frac{\psi^2(\xi)}{2c} \tag{113}$$

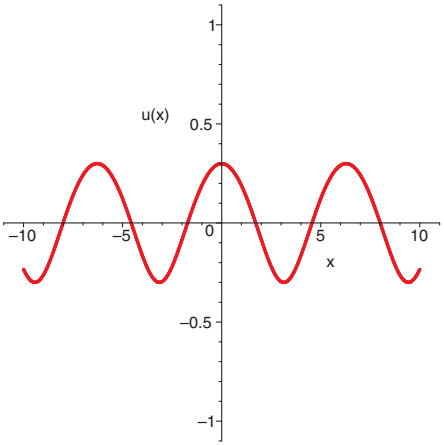

(a) $h = 0.36$

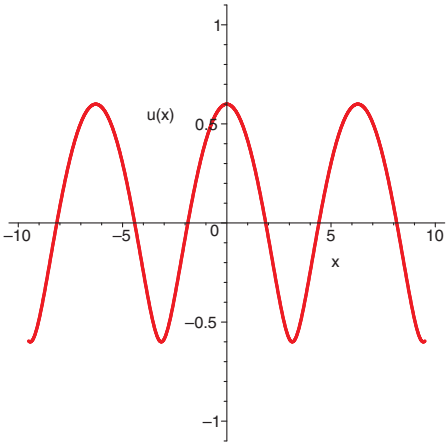

(b) $h = 1.44$

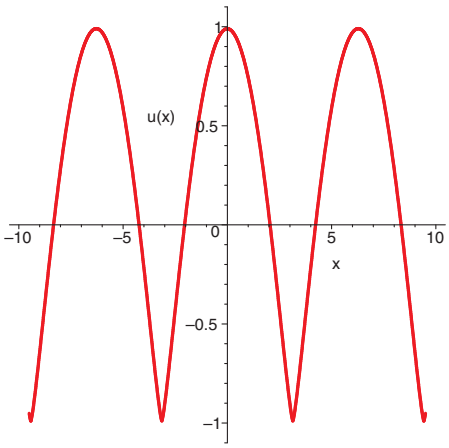

(c) $h = 4$

Figure 15. When $\lambda < 0, a < 0, c < 0$, as h from 0 tends to $h_c = -4ac^2$, the smooth periodic waves evolve into a singular periodic wave.

and

$$2\sqrt{-\psi^2 - 2c\psi} - \arctan\left(\frac{\psi + c}{\sqrt{-\psi^2 - 2c\psi}}\right) = -\frac{2\sqrt{c\lambda}}{\lambda}|\xi - 2nT_9| - \pi. \quad (114)$$

For $\lambda > 0, a > 0, c > 0$, we may have similar results mentioned above. Under those parameter conditions, the phase portrait of the system (100) and periodic waves of the DHS Equation (18) are shown in Figures 14(b) and 16, respectively.

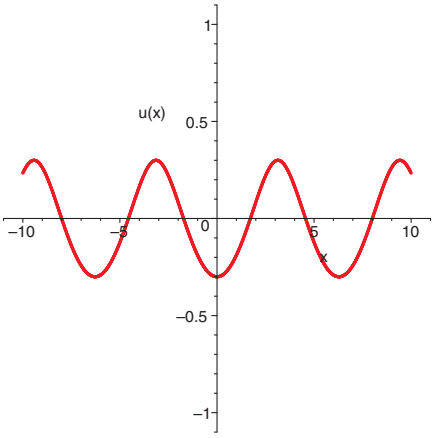

(a) $h = -0.36$

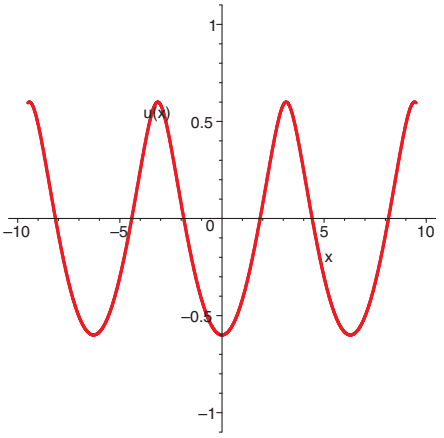

(b) $h = -1.44$

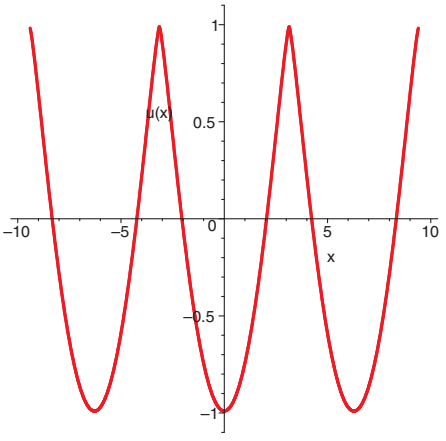

(c) $h = -4$

Figure 16. When $\lambda > 0, a > 0, c > 0$, as h from 0 tends to $h_c = -4ac^2$, the smooth periodic waves evolve into a singular periodic wave.

6. Conclusion and discussion

In this paper, we study the effects of quadratic singular curves in integrable wave equations by using the bifurcation theory of dynamical system. To compare the difference between the effects of singular straight lines and the effects of quadratic singular curves in the integrable wave equations, we first recall the occurrence of peakon and cuspon through the phase space analytical technique. Then it is followed by several specific nonlinear wave equations as examples to discuss the effects of quadratic singular curves. As shown in the previous

sections, there exists a close connection between those singular traveling waves and quadratic singular curves in phase plane. We present some new singular solitary waves and singular periodic waves for some integrable wave equations, which possess more weaker singularity than the classical singular traveling waves such as peakon, cuspon, and cusped periodic wave. It is shown that the second derivative of the new singular solitary wave and singular periodic wave solutions does not exist at their crests where the first derivative does exist.

Equations (25) and (34) have physical background and actually coincide with the Newton equation of a particle in the potential

$$V_1(\varphi) = \varphi^2 - \frac{32c^2}{27(\varphi - c)}, \quad V_2(\varphi) = \varphi^2 + 2\sqrt{4a^2 - a\varphi^2}, \text{ respectively.}$$

Thus, we solve the Newton equation $\varphi_\xi^2 = V_1(\varphi) - V_1(A)$ for cuspon solutions and $\varphi_\xi^2 = V_2(\varphi) - V_2(0)$ for pseudo-cuspon solutions, where $A = -\frac{c}{3}$. This is very helpful for us to deal with physical equations. The singular solitary wave solutions are expected to apply in nonlinear shallow-water wave theory and Newton motion theory because they have a very close relation to the Newton Equations (25) and (34).

We study the qualitative and analytic behaviors of the pseudo-cuspon solution and singular periodic wave solutions by theoretical analysis and numerical simulation, but stability of pseudo-cuspon and compacton of those equations is not clear yet.

Acknowledgments

This work are supported by the National Natural Science Foundation of China (No. 11161013, No. 11361017, No. 11171295, No. 61301187, and No. 61328103) and Foundation of Guangxi Key Lab of Trusted Software.

The authors wish to thank the anonymous reviewers for their helpful comments and suggestions. A. Chen sincerely thanks Prof. Jibin Li for his kind help. Z. Qiao also thanks the U.S. Department of Education GAANN project (P200A120256) to support UTPA mathematics graduate program, and the China state administration of foreign experts affairs system under the affiliation of China University of Mining and Technology.

References

1. C. Rogers and W. R. Shadwick, *Bäcklund Transformation and Their Applications*, Academic, New York, 1982.
2. W. Malfliet and W. Hereman, The tanh method: I. Exact solutions of nonlinear evolution and wave equations, *Phys. Scripta*. 54: 563–568 (1996).
3. R. Hirota, *Direct Method in Soliton Theory*, Springer, Berlin, 1980.

4. J. S. Cohen, *Computer Algebra and Symbolic Computation: Mathematical Methods*, AK Peters, Ltd., Natick, MA 07160, USA, 2003. [ISBN 978-1-56881-159-8]
5. S. Lie, Uber die integration durch bestimmte integrale von einer klasse linearer partieller differential eichungen, *Arch. Math.* 6: 328–368 (1881).
6. H.-H. Dai, *Exact travelling-wave solutions of an integrable equation arising in hyperelastic rods*, *Wave Motion* 28: 367–381 (1998).
7. H.-H. Dai and X.-H. Zhao, Nonlinear Traveling waves in a rod composed of a modified Mooney-Rivlin material I: Bifurcation of equilibra and non-singular case, *Proc. R. Soc. Lond. A: Math. Phys. Eng. Sci.* 455: 3845–3874 (1999).
8. J. Li and Z. Liu, Smooth and non-smooth travelling waves in a nonlinearly dispersive equation, *Appl. Math. Model.* 25: 41–56 (2000).
9. Z. Liu and T. Qian, Peakons of the Camassa-Holm equation, *Appl. Math. Model.* 26: 473–480 (2002).
10. H.-H. Dai, D. B. Huang, and Z. R. Liu, Singular dynamics with application to singular waves in physical problems, *J. Phys. Soc. Japan* 73: 1151–1155 (2004).
11. J. Li and G. Chen, On a class of singular nonlinear traveling wave equations, *Int. J. Bifurc. Chaos* 17: 4049–4065 (2007).
12. D. Feng and J. Li, Exact explicit travelling wave solutions for the (n+1)-dimensional ϕ^6 field model, *Phys. Lett. A*. 369: 255–261 (2007).
13. W. Rui, B. He, Y. Long, and C. Chen, The integral bifurcation method and its application for solving a family of third-order dispersive PDEs, *Nonlinear Anal.* 69: 1256–1267 (2008).
14. J. Li and Z. Qiao, Bifurcations of traveling wave solutions for an integrable equation, *J. Math. Phys*. 51: 042703–09 (2010).
15. A. Chen and J. Li, Single peak solitary wave solutions for the osmosis K(2,2) equation under inhomogeneous boundary condition, *J. Math. Anal. Appl.* 369: 758–766 (2010).
16. H.-H. Dai and F. F. Wang, Asympotic bifurcation solutions for compressions of a clamped nonlinearly elastic rectangle: Transition region and barrelling to a corner-like profile, *SIAM J. Appl. Math.* 70: 2673–2692 (2010).
17. J. Yang, Classification of solitary wave bifurcations in generalized nonlinear Schrödinger equations, *Stud. Appl. Math.* 129: 133–162 (2012).
18. R. Camassa and D. Holm, An integrable shallow wave equation with peaked solitons, *Phys. Rev. Lett.* 71: 1661–1664 (1993).
19. P. Rosenau, On nonanalytic solitary waves formed by a nonlinear dispersion, *Phys. Lett. A*. 230: 305–318 (1997).
20. P. Rosenau and J. M. Hyman, Compactons: Solitons with finite wavelengths, *Phys. Rev. Lett.* 70: 564–567 (1993).
21. L. Zhang, L. Chen, and X. Hou, The effects of horizontal singular straight line in a generalized nonlinear Klein-Gordon model equation,*Nonlinear Dyn*. 72: 789–801 (2013).
22. J. Zhou, L. Tian, and X. Fan, New exact travelling wave solutions for the K(2,2) equation with osmosis dispersion, *Appl. Math. Comput.* 217: 1355–1366 (2010).
23. J. Zhou, and L. Tian, Soliton solution of the osmosis K(2,2) equation, *Phys. Lett. A.* 372: 6232–6234 (2008).
24. Q. Bi, Peaked singular wave solutions associated with singular curves, Chaos, *Solitons Fractals* 31: 417–423 (2007).
25. Z. Liu, Q. Li, and Q. Lin, New bounded travelling waves of Camassa-Holm equation, *Int. J. Bifurc. Chaos* 14: 3541–3556 (2004).
26. Z. Liu and B. Guo, Periodic blow-up solutions and their limit forms for the generalized Camassa-Holm equation, *Progr. Nat. Sci.* 18: 259–261 (2008).

27. J. Shen and W. Xu, Bifurcations of smooth and non-smooth travelling wave solutions in the generalized Camassa-Holm equation, *Chaos, Solitons Fractals* 26: 1149–1162 (2005).
28. J. Lenells, Traveling wave solutions of the Camassa-Holm equation, *J. Different. Equat.* 217: 393–430 (2005).
29. Z. Qiao and G. Zhang, On peaked and smooth solitons for the Camassa-Holm equation, *Europhys. Lett.* 73: 657–663 (2006).
30. A. Chen, J. Li, C. Li, and Y. Zhang, From bell-shaped solitary wave to W/M-shaped solitary wave solutions in an integrable nonlinear wave equation, *Pramana-J. Phys.* 74: 19–26 (2010).
31. Z. Qiao, A new integrable equation with cuspons and W/M-shape peaks solitons, *J. Math. Phys*. 47: 112701–112709 (2006) and New integrable hierarchy, parametric solutions, cuspons, one-peak solitons, and M/W-shape peak solutions, *J. Math. Phys.* 48:082701-082720 (2007).
32. J. Li and Z. Qao, Bifurcations and exact traveling wave solutions for a generalized Camassa-Holm equation, *Int. J. Bifurc. Chaos* 23 : 1350057–1–17 . (2013).
33. J. Li, X. Zhao, and G. Chen, Breaking wave solutions to the second class of singular nonlinear traveling wave equations, *Int. J. Bifurc. Chaos* 19: 1289–1306 (2009).
34. P. J. Olver and P. Rosenau, Tri-Hamiltonian duality between solitons and solitary-wave solutions having compact support, *Phys. Rev. E.* 53: 1900–1906 (1996).
35. A. Chen and S. Wen, Double compactons in the Olver-Rosenau equation, Pramana, *J. Phys.* 80: 471–478 (2013).
36. A. S. Fokas, On class of physically important integrable equations, *Physica D* 87: 145–150 (1995).
37. J. Li and J. Zhang, Bifurcations of traveling wave solutions in generalization form of the modified KdV equation, *Chaos Solitons Fractals* 20: 899–913 (2004).
38. Q. Bi, Singular solitary waves associated with homoclinic orbits, *Phys. Lett. A*. 352: 227–232 (2006).
39. M. A. Manna and A. Neveu, A singular integrable equation from short capillary-gravity waves, preprint arXiv: physics/0303085 (2003).
40. J. C. Brunelli, A. Das, and Z. Popowicz, Deformed Harry Dym and Hunter-Zheng equations, *J. Math. Phys.* 45: 2646–50 (2004).
41. A. Chen, Y. Lin, and S. Li, Bifurcation studies on travelling wave solutions for an integrable nonlinear wave equation, *Appl. Math. Comput*. 216: 611–622 (2010).
42. A. Chen, W. Huang, and J. Li, Qualitative behavior and exact travelling wave solutions of the Zhiber-Shabat equation, *J. Comput. Appl. Math.* 230: 559–569 (2009).
43. Z. Qiao and X Q. Li, An integrable equation with non-smooth solitons, *Theoret. Math. Phys.* 167: 584–589 (2011).
44. Z. Qiao, B. Q. Xia, and J. Li, Integrable system with peakon, weak kink, and kink-peakon interactional solutions, 2012, arXiv:1205.2028v2 [nlin.SI].
45. J. K. Hunter and R. Saxton, Dynamics of director fields, *SIAM J. Appl. Math.* 51: 1498–1521 (1991).
46. Z. Qiao, New hierarchies of isospectral and non-isospectral integrable NLEEs derived from the Harry-Dym spectral problem, *Physica A* 252: 377–387 (1998).

Guilin University of Electronic Technology
Hezhou University
University of Texas-Pan American

(Received September 10, 2013)